UMEÅ UNIVERSITY MEDICAL
DISSERTATIONS

New series No. 1160

Biomechanical assessment of head and neck movements in neck pain using 3D movement analysis

Helena Grip

Department of Radiation Sciences, Umeå University, Sweden,
and
Department of Biomedical Engineering and Informatics, Umeå University Hospital, Umeå, Sweden.

Umeå 2008

Front cover:
Posture. © Helena Grip 2008.

ISSN: 0346-6612
ISBN: 978–91–7264–518-9

Printed by Print & Media: 2004281
Umeå University, Sweden, 2008

We are still confused,
But on a much higher level

Winston Churchill

Abstract

Three-dimensional movement analysis was used to evaluate head and neck movement in patients with neck pain and matched controls. The aims were to further develop biomechanical models of head and neck kinematics, to investigate differences between subjects with non-specific neck pain and whiplash associated disorders (WAD), and to evaluate the potential of objective movement analysis as a decision support during diagnosis and follow-up of patients with neck pain.

Fast, repetitive head movements (flexion, extension, rotation to the side) were studied in a group of 59 subjects with WAD and 56 controls. Angle of rotation of the head was extracted using the helical axis method. Maximum and mean angular velocities in all movement directions were the most important parameters when discriminating between the WAD and control group with a partial leas squares regression model. A back propagation artificial neural network classified vectors of collected movement variables from each individual according to group membership with a predictivity of 89%.

The helical axis for head movement were analyzed during a head repositioning, fast head movements and ball catching in two groups of neck pain patients (21 with non-specific neck pain and 22 with WAD) and 24 matched controls. A moving time window with a cut-off angle of 4° was used to calculate finite helical axes. The centre of rotation of the finite axes (CR) was derived as the 3D intersection point of the finite axes. A downward migration of the axis during flexion/extension and a change of axis direction towards the end of the movements were observed. CR was at its most superior position during side rotations and at its most inferior during ball catching. This could relate to that side rotation was mainly done in the upper spine, while all cervical vertebrae were recruited to stabilize the head in the more complex catching task.

Changes in movement strategy were observed in the neck pain groups: Neck pain subjects had lower mean velocities and ranges of movements as compared with controls during ball catching, which could relate to a stiffer body position in neck pain patients in order to stabilize the neck. In addition, the WAD group had a displaced axis position during head repositioning after flexion, while CR was displaced during fast side rotations in the non-specific neck pain group. Pain intensity correlated with axis and CR position, and may be one reason for the movement strategy changes.

Increased amount of irregularities in the trajectory of the axis was found in the WAD group during head repositioning, fast repetitive head movements and catching. This together with an increased constant repositioning error during repositioning after flexion indicated motor control disturbances. A higher group standard deviation in neck pain groups indicated heterogeneity among subjects in this disturbance.

Wireless motion sensors and electro-oculography was used simultaneously, as an initial step towards a portable system and towards a method to quantify head-eye co-ordination deficits in individuals with WAD. Twenty asymptomatic control subjects and six WAD subjects with eye disturbances (e.g. dizziness and double vision) were studied. The trial-to-trial repeatability was moderate to high for all evaluated variables (intraclass correlation coefficients >0.4 in 31 of 34 variables). The WAD subjects demonstrated decreased head velocity, decreased range of head movement during gaze fixation and lowered head stability during head-eye co-ordination as possible deficits.

In conclusion, kinematical analyses have a potential to be used as a support for physicians and physiotherapists for diagnosis and follow-up of neck pain patients. Specifically, the helical axis method gives information about how the movement is performed. However, a flexible motion capture system (for example based on wireless motion sensors) is needed. Combined analysis of several variables is preferable, as patients with different neck pain disorders seem to be a heterogeneous group.

Original papers

This dissertation is based on the following papers, which are referred to by their Roman numbers in the text. Papers I-III are reprinted with permission from the publishers.

I. Öhberg F, Grip H, Wiklund U, Sterner Y, Karlsson JS, Gerdle B, Chronic Whiplash Associated Disorders and Neck Movement Measurements: An Instantaneous Helical Axis Approach. *IEEE Trans Inf Tech BioMed*, 2003; 274-282

II. Grip H, Öhberg F, Wiklund U, Sterner Y, Karlsson JS, Gerdle B, Classification of Neck Movement Patterns related to Whiplash-Associated Disorders using Neural Networks. *IEEE Trans Inf Tech BioMed*, 2003; 412-418

III. Grip H, Sundelin G., Gerdle B, Karlsson JS, Variations in the axis of motion during head repositioning – A comparison of subjects with whiplash-associated disorders or non-specific neck pain and healthy controls. *Clin Biomech (Bristol, Avon)*, 2007; 22: 865-73

IV. Grip H, Sundelin G., Gerdle B, Karlsson JS, Cervical helical axis characteristics and its centre of rotation during active head movements - comparisons of whiplash-associated disorders, non-specific neck pain and asymptomatic individuals. *Submitted*

V. Grip H, Jull G, Treleaven J, Head eye co-ordination and gaze stability using simultaneous measurement of eye in head and head in space movements – potential for use in subjects with a whiplash injury. *Submitted*

List of abbreviations

Vectors are written in bold, small letters, matrices in bold capital letters and scalar numbers in cursive text.

ANN	Artificial neural networks
ANOVA	Analysis of variance
BP	Back propagation (training algorithm for artificial neural networks, ANN)
BPNN	Back propagation neural networks
c	the 3D position of the point on the helical axis (axis of motion) that is closest to origo (see IHA)
CON	control subject
DOF	Degrees of Freedom
EOG	Electro-oculography
EMG	Electromyography
CR	the Centre of the axis of rotation i.e. the 3D intersection point of a set of helical axes
CT	Computed tomography - medical imaging method
FHA	Finite helical axis method – an approximation of the instantaneous helical axis (IHA) during finite intervals.
ICC	Intraclass correlation coefficients (statistical method to evaluate reliability of repeated measures)
ICR	Instantaneous centre of rotation
IHA	Instantaneous helical axis method – a 6 degree-of-freedom model that describes the movement of a rigid body as a positive rotation around a freely moving axis.
IAR	Instantaneous axis of rotation
MRI	Magnetic Resonance Imaging - visualize the structure and function of the body
n	the direction vector of the helical axis (axis of motion)
NP	non-specific neck pain
PCA	Principal component analysis
PLS	Partial least squares regression

R	the rotation matrix – a general description of the 3D rotation in space of a rigid body
ROM	Range of Movement
QTF	Scientific Monograph of the Quebec Task Force on Whiplash Associated Disorders
SVD	Singular value decomposition
t	the scalar translation of the rigid body along the helical axis (axis of motion, see IHA)
v	the translation vector – a general description of the 3D translation in space of a rigid body
VIP	Variable influence on projection
WAD	Whiplash associated disorders
θ	the helical angle of rotation around the helical axis (axis of motion)
ω	The 3D-angle between **n** and a reference position $\mathbf{n}_{ref}$
α	The first Euler angle
β	The second Euler angle
γ	The third Euler angle

Contents

1 Introduction

The understanding of head and neck movements is important both when investigating neck injuries and for follow-up of neck pain patients. A change in an individual's neck movement pattern can result from disturbances in proprioception, disturbances of the vestibular system, from changes in movement strategy due to pain or from physical changes in the joints and musculature. Hence, a detailed description of neck movement characteristics is very important for the understanding of neck disorders.

The head and neck system consists of seven vertebrae and is a complex system from a kinematical point of view. Analysis of individual joints can be used to identify or describe changes in function and disc stiffness of a single joint. Normally, the spine mainly functions as a coupled unit, and neck kinematics can be analysed by studying head movement relative to the upper body. In this dissertation, characteristics of the neck as a whole were studied in individuals with neck pain and in asymptomatic individuals.

An introduction to the anatomy of the neck with focus on biomechanics is given in Chapter 2 to explain how the movement of the head results from a combined movement of the cervical vertebrae. A short medical background on two medical conditions that involve neck pain (non-specific neck pain and whiplash associated disorders) and some possible mechanisms and rehabilitation implications are given in Chapter 3. Different kinematic models (such as the Euler and the Helical axis method) are described in Chapter 4, and different movement registration systems are presented in Chapter 5. These descriptions point out the advantages and disadvantages with the chosen models and methods.

Pattern classification (neural networks and partial least squares regression) were used to classify neck movements, and are therefore described in Chapter 6.

Finally, the studies included in this thesis and the resulting five papers are described and discussed in Chapters 7-11.

2 Anatomy and biomechanics of head and neck

The neck and shoulder region consists of several complex muscle arrangements and multi-segmental cervical joints that move and stabilize the head and neck. Neuronal pathways run through the neck and are involved in daily functions such as speech, vision, swallowing and breathing. For example, cervical nerve afferents project to the superior colliculus, which is a reflex centre for co-ordination between head and neck movement (Corneil et al., 2002; Werner, 1980) and are also involved in reflex responses for gaze stability when moving the head (Mergner et al., 1998). However, this chapter focuses on the biomechanics of the cervical spine.

2.1 Earlier work

Ranges of movement and axis of rotation for single vertebrae during flexion, extension, side rotation and lateral bending have been examined in a number of studies, as reviewed by White and Panjabi (White and Panjabi, 1978). Until recently, most studies have been done on cadaver spines or have been based on X-ray or computed tomography (Table 2.1). The instantaneous axis or centre of rotation, IAR or ICR have been used to estimate the 2D or 3D position of the rotation axis during flexion and extension (Amevo et al., 1991; Hinderaker et al., 1995; Lee et al., 1997; Penning, 1978). In vivo measurements of the cervical spine without risk for the subject, such as optical movement analysis, were introduced in the beginning of 1990. This made it possible to do more accurate 3D estimates of the rotation axis by using the Helical axis method (Woltring et al., 1994). Most commonly the global spine movements, head relative to the body, have been studied in vivo.

Table 2.1 A summary of relevant work on the biomechanics of the head and cervical spine.

Study	Methods/variables	Subjects	Main findings
(Penning, 1978)	IAR* for maximal flexion/extension, side rotation and lateral bending in cervical vertebrae.	25 normal young adults.	Descriptions of individual vertebrae. Side rotation mainly by C1/C2. Coupled movement in lower cervical vertebrae. Combined upper extension/lower flexion and vice versa may occur.
(Penning and Wilmink, 1987)	IAR from Computed tomography during maximal side rotations, in cervical vertebrae.	26 normal young adults.	Maximal degree range of motion in C0/C1 to C7/T1 is 1.0, 40.5, 3.0, 6.5, 6.8, 6.9, 5.4, and 2.1°. IAR is in the sagittal plane, passing through the front of the moving vertebra.
(Amevo et al., 1991)	IAR* for maximal flexion/extension in cervical vertebrae.	40 normal subjects.	Normal range of locations for IAR. The biological variations and technical errors were low.
(Amevo et al., 1992)	IAR* for maximal flexion/extension in cervical vertebrae.	109 subjects, uncomplicated neck pain.	Unequivocally abnormal IAR in 46% and marginally abnormal in 26% of subjects with neck pain.
(Winters et al., 1993)	Video cameras and a head cluster of five markers. The finite helical axis for intervals of 10°	9 normal subjects, 18 subjects with neck injury. Tested twice within a 6-week interval.	Vertical axis during side rotation. Lateral axis at level C3-T1 during flex./ext. Some individuals with neck injury have extreme high or low axis positions.
(Milne, 1993)	IAR* of cadaver spines during axial rotation and lateral bending.	Cadaver normal cervical spines from 22 subjects.	Axis passes through front of disc and posterior part of moving vertebra. Axis variation larger in lower than upper cervical spine.

* IAR: superimposing 2 radiographic films of two different positions of a vertebra to calculate the instantaneous axis of rotation of this vertebra

Continue **Table 2.**

Study	Methods/variables	Subjects	Main findings
(Woltring et al., 1994)	Video cameras and four-marker clusters, head and upper body. Tracking the instantaneous helical axis at 60 Hz, low-pass filter at 0.375 Hz.	One WAD subject (F, 30 yr) before and after treat-ment. One control subject (M, 52 yr).	Scattered movement of IHA during flex/ext. in a WAD subject before treatment.
(Hinderaker et al., 1995)	Correlation of IAR* of the C2-3 segment with diagnostic blocks of the C2-3 facet joint.	82 patients with headache of cervical origin. IAR could only be determined in 54 patients.	No significant correlation between IAR and the response to diagnostic blocks.
(Lee et al., 1997)	The instantaneous centre of rotation (i.e. IAR) of head relative to upper body at 10° intervals of flexion and extension, using an goniometric method.	27 controls, 28 with spondylosis and 17 with cervical disc degeneration.	Anterior displacement of the IAR during flex./ext. in patients with spine instability.
(Feipel et al., 1999)	Head relative to upper body using an electro-goniometric method.	250 healthy subjects (age 14 -70 yr).	ROM 144±20° side rotation, 122 ±20° flex/ext. Decreases with age. No difference between men and women
(Ishii et al., 2004)	Three-dim MRI of the upper cervical spine in 15° intervals during side rotation (Euler angles).	15 healthy subjects.	Confirms coupled lateral bending with axial rotation
(Senouci et al., 2007)	Three-dim motion analysis of side rotation. Mathematical relationships between side rotation and lateral bending.	40 healthy subjects.	Quantifies coupled lateral bending with axial rotation (e.g. 80° side rotation is coupled with approximately 10° lateral bending).

* IAR: superimposing 2 radiographic films of two different positions of a vertebra to calculate the instantaneous axis of rotation of this vertebra

2.2 The cervical spine

The spine, or vertebral column, is divided into four regions: the cervical (7 vertebrae), thoracic (12 vertebrae), lumbar (5 vertebrae) and the sacral-coccyx region (9 fused vertebrae). Any change in spine posture involves a coupled movement of the joint segments, and kinematics of the spine deals with either single segments or an entire region of the spine. To analyse individual segments, individual co-ordinate systems must be defined since not all segments are horizontal. For example, axial rotation of the head does not correspond to axial rotation in each individual spine segment (Zatsiorsky, 1998).

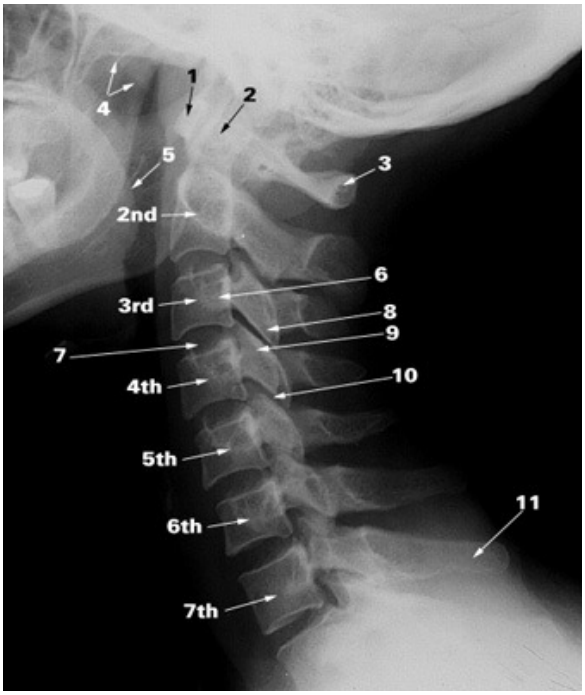

Figure 2.1. Lateral view of the cervical spine, showing the 2nd to 7th cervical vertebrae. The anterior (1) and posterior (3) arch of atlas, the dens of C2 (2), inferior (8), superior (9), and transverse (6) articular processes, a facet joint (10), a disc (7), and the spinous processes of C7 (11) are indicated. Re-printed with permission from the Department of Radiology, University of Szeged, Hungary, http://www.szote.u-szeged.hu/Radiology/ Anatomy/skeleton/ neck1.htm.)

2.2.1 Upper cervical spine

The upper cervical spine consists of two vertebrae. The first, atlas, is a ring of bone holding up the head. The second vertebra, axis, has a peg called dens that projects through the atlas, and makes a pivot on which the atlas and head rotate during side rotations. The two vertebrae and the head form two joints: the occipital-atlantal (C0/C1) and the atlanto-axial (C1/C2) joint. The range of movement of each joint is illustrated in Table 2.2. Flexion and extension take place in both joints, while lateral bending occurs in the occipital-atlantal joint and axial rotation occurs in the atlanto-axial joint (Zatsiorsky, 1998). The atlanto-axial joint is responsible for more than 50% of the total range of side rotation. The motion is screw-like, since C1 translates downwards as it rotates (Zatsiorsky, 1998).

2.2.2 Lower cervical spine

The vertebrae of the lower spine all have similar geometry, with equally distributed range of movement that allows flexion-extension, side rotation and lateral bending (Table 2.2).

Table 2.2. Range of movement (°) of the cervical segments for maximal flexion/extension, lateral bending, and side rotation from left to right.

Segment	Flexion/Extension		Lateral bending	Side rotation
	A	B	B	C
C0/C1	Not studied	30		1
C1/C2	Not studied	30	10	40.5
C2/C3	11 ± 3.4	12		3.0
C3/C4	15 ± 4.0	18		6.5
C4/C5	17 ± 4.6	20	70	6.8
C5/C6	17 ± 6.1	20		6.9
C6/C7	14 ± 4.7	15		5.4

[A] Amevo et al, 1992

[B] Penning, 1978

[C] Penning and Wilmink, 1987

Each vertebra consists of a vertebral body, a vertebral foramen through which the spinal cord runs, superior articular facets on each side of the foramen, and the spinous process on the back of the vertebra (Fig. 2.1). Each motion segment consists of two adjacent vertebrae and the disc in between. This result in three joints per segment: the intervertebral joint between the vertebral bodies and the disc and two facet joints between the articular processes. This makes the spine both stable and flexible (Tortora and Grabowski, 2000). The intervertebral disc function as a shock absorber between the vertebrae, and its deformation enables small translations of each segment (Zatsiorsky, 1998). Since the movement is guided by facet joints, lateral bending and rotation are always combined (Ishii et al., 2004; Penning, 1978; Senouci et al., 2007). This coupling between side rotation and side bending can be visualized with the axis of rotation, also called axis of motion, Fig. 2.2.A.

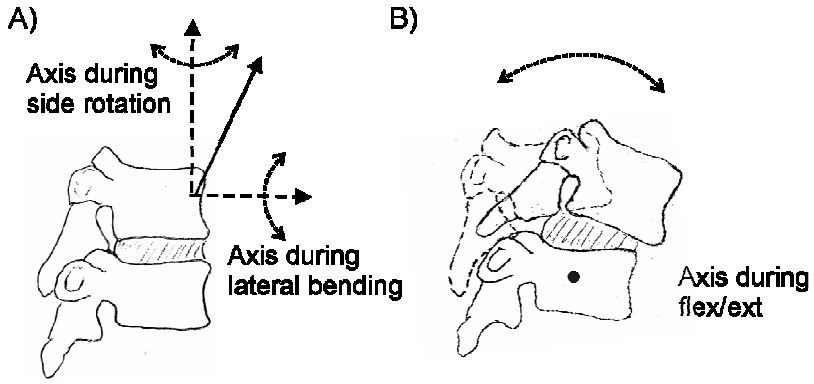

Fig. 2.2A-B. The instantaneous axis of rotation in a cervical segment depends on the type of movement. In A), coupled lateral bending and side rotation of the vertebrae gives an axis that passes through the front of the moving vertebrae and points upwards/forward (Milne, 1993; Penning and Wilmink, 1987). In B, flexion and extension of the vertebra gives an axis that is horizontal, passing through the lower vertebra. (Amevo et al., 1992). The axis position is marked with a dot.

The composite axis of motion from all cervical vertebrae describes the head movement relative to the upper body. It is also

directed upwards/backwards during side rotations, and it is positioned slightly off-centre: to the right during right side rotations and vice versa (Winters et al., 1993).

The planar position of this axis can be used to describe the movement of individual spine segments. One way is to superimpose radiographs from flexion and extension and construct perpendicular bisectors from the segment surfaces. The point of intersection of these bisectors is called the instantaneous axis of rotation, IAR (Amevo et al., 1992; Amevo et al., 1991; Hinderaker et al., 1995; Penning and Wilmink, 1987; Qiu et al., 2004). The use of the word "instantaneous" refers to that the location depends on the set of positions that are compared. In a normal cervical spine, IAR lies in the vertebral body below the moving vertebra during flexion/extension (Fig. 2.3). If a spine segment does not function properly, its IAR may be displaced (Amevo et al., 1992), which can lead to compression of facet joint surfaces (Zatsiorsky, 1998).

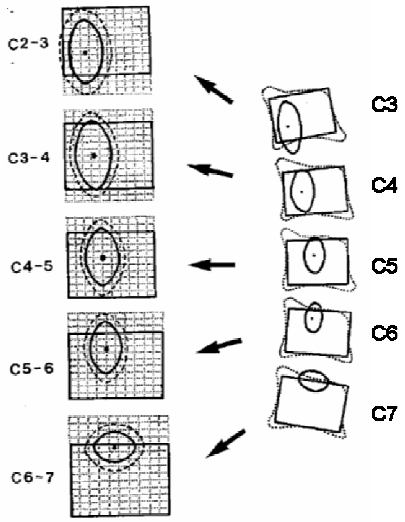

Fig. 2.3. The instantaneous axes of rotation during maximal flexion/extension for cervical vertebrae. The mean position of each IAR is indicated with a dot and the standard deviation with an oval. Modified with permission from (Amevo et al., 1992).

2.3 Musculature of neck and shoulders

The static and dynamic control of the head and neck is managed by a complex arrangement of about 20 muscles that enclose the cervical spine (Fig. 2.4).

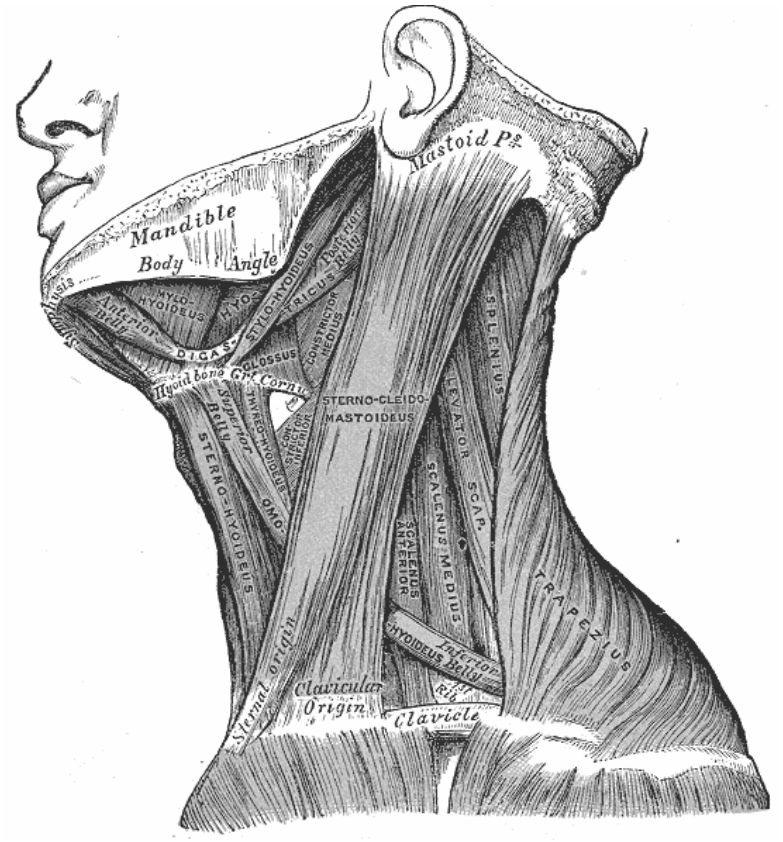

Fig. 2.4 Illustrates musculature of head and neck. Sternocleidomastoideus is positioned along the lateral side of the neck and trapezius on the back of the neck and upper back/shoulders. Re-printed from (Gray, 1918) .[1]

[1] This figure was originally published in 1918, and therefore has now lapsed into the public domain

The muscles at the upper cervical spine have individual specialised arrangement, enabling lateral bending in C0/C1 and side rotation in C1/C2. Normally, the first 45° of rotation occurs in C1/C2, and then the lower cervical spine becomes involved (Zatsiorsky, 1998). On the contrary, the muscles in the lower cervical spine are coherent or interwoven, with every muscle activating several segments (Kamibayashi and Richmond, 1998; Penning, 1978). This causes the segments of the lower spine to act as one unit.

Anatomically, the deeper muscles are related intimately with the cervical osseous and articular elements (and thereby have a stabilizing function), whereas the superficial muscles have no attachments to the cervical vertebrae (Kamibayashi and Richmond, 1998). The deep musculature has a very high spindle density (Boyd-Clark et al., 2002; Kulkarni et al., 2001). The muscle spindles mediates the proprioceptive inputs from the cervical musculature and have an important role in head-eye coordination and postural control (Tortora and Grabowski, 2000). The musculature involved in head and neck movement and stabilization of head and neck is presented in Table 2.3.

Table 2.3 Musculature of the neck and back that is involved in head and neck movement (Putz and Pabst, 1994a, 1994b; Tortora and Grabowski, 2000).

Muscle	Function
Muscles of the neck, Mm. colli	
Sternocleidomastoideus	Supports the head Extension C0/C1 [b] Side rotation[uo]
Lateral vertebral muscles Scalenus anterior Scalenus medius Scalenus posterior	Lateral bending of the cervical spine
Anterior vertebral muscles Longus colli Longus capitis	Flexion[b] Lateral bending [us] Side rotation [us]
Suboccipital muscles Rectus capitis Obliquus capitis	Extend and rotate the head Flexion of head (*rectus c.*) Side bending of head[us] (*rectus c.)*
Muscles of the back, M. dorsi	
Upper trapezius	Elevates the scapula Function together with other muscles; seldom as a single unit
Superficial erector spinae muscles Ilicostalis cervicis Longissimus cervicis Longissimus capitis Spinalis cervicis Spinalis capitis	Maintaining erect posture[b] Lateral bending[us] Extension[b]
Superficial muscles Splenius capitis Splenius cervicis	Rotates the head Rotation and lateral bending of the cervical spine
Deep transverso-spinales muscles Semispinalis cervicis Semispinalis capitis	Supports the head Extension of head (C0/C1) and cervical spine
Mm. Multifidi Mm. rotares cervicis	Stabilize individual segments Lateral bending [us] Side rotation [us]

[b] bilaterally action, [us] unilateral contraction on the same side as the movement, [uo] unilateral contraction on the side opposite to the movement

3 Neck and shoulder pain

Neck- and back disorders are a growing problem with significant individual suffering and high costs to society. Neck pain may arise from any of the structures in the neck: the intervertebral discs, ligaments, muscles, facet joints, dura and nerve roots (Bogduk, 1988). Hence, there are a large number of potential causes of neck pain. These vary between tumours, traumas, infection, inflammatory disorders and congenital disorders. In most cases, no systematic disease can be detected as the underlying cause of the complaints, and the condition is then often referred to as "non-specific neck pain" (Bogduk, 1984, 1988; Borghouts et al., 1998). Neck trauma from acceleration and deceleration forces acting on the head, such as a rear-end car crashes, can result in the medical condition categorized as whiplash-associated disorders, WAD (Spitzer et al., 1995).

3.1 Non-specific neck pain

In the majority of cases of neck pain, no specific cause can be identified (Bogduk, 1984, 1988; Borghouts et al., 1998). In many cases it is believed that the pain is work related, with static workload and uncomfortable working postures as underlying causes (Bernard, 1997; Fjellman-Wiklund and Sundelin, 1998; Sundelin and Hagberg, 1992), but also psychosocial risk factors have been reported as contributors (Ariens et al., 2001). There are indications that the localization of pain (such as radiation to the arms or neurological signs) and radiological findings (such as degenerative changes in the discs and joints) are not associated with a worse prognosis. Instead, a higher severity of pain and a greater number of previous attacks seem to be associated with a worse prognosis (Borghouts et al., 1998; Scholten-Peeters et al., 2003).

3.2 Whiplash associated disorders

The term whiplash injury was introduced by Crowe in 1928, when he described the whiplash-like effect on the neck and upper body caused by rear-end vehicle accidents (Crowe, 1928). The Scientific Monograph of the Quebec Task Force on Whiplash Associated Disorders (QTF) in 1995 adopted the following definition (Spitzer et al., 1995):

> *Whiplash* is an acceleration-deceleration mechanism of energy transfer to the neck. It may result from rear or side impact motor vehicle, but can occur during diving or other mishaps. The impact can lead to a variety of clinical manifestations (*Whiplash associated disorders, WAD*).

Today, the incidence of WAD varies between 0.8-4.2 per thousand inhabitants and per year (Carlsson et al., 2005). Although the majority becomes asymptomatic in a matter of weeks to a few months, 20 to 40 percent have long term symptoms that persist more than 3 months (Carlsson et al., 2005). Currently, the model by the Quebec Task Force is mostly used to classify WAD (Spitzer et al., 1995), Table 3.1.

Table 3.1. Quebec task force classification of WAD

Grade	Definition
1	Neck pain but no musculoskeletal or neurological signs
2	Neck pain and musculoskeletal signs (sore muscles, decreased range of motion)
3	Neck pain and neurological signs (loss of motor activity, impaired sensory function
4	Neck pain and fractures or dislocations

The WAD patients that come to the clinic often have WAD grades 2-3 (as reviewed by Sterner and Gerdle, 2004). Symptoms that can be present in all grades are dizziness, headache, memory loss, difficulties with swallowing (dysphagia), tinnitus and temporomandibular joint pain. Commonly, patients have pain in the trapezius and sternocleidomastoideus muscles (Fig. 2.4). Many clinical symptoms are prevalent both in the acute and chronic phases of WAD, for example headache, stiffness and pain in the neck, paraesthesiae (i.e., abnormalities of sensation) or weakness in arms, visual and auditory disturbance.

There is no current consensus among researchers about the injury mechanism behind the symptoms. During a rear-impact, both the upper and lower cervical spine are at risk for extension injury (Panjabi et al., 2004). The C1/C2, C5/C6 and C6/C7 segments are the most frequently injured segments (Taylor and Taylor, 1996). Subtle lesions on intervertebral discs and injuries on facet joints are more common than injuries on the vertebral bodies, and most lesions cannot be seen on radiographs (Taylor and Taylor, 1996).

3.3 Heterogeneity in neck pain groups

The main symptoms, pain and stiffness in neck and shoulders, are the same for non-specific neck pain and long-term WAD. Some studies report that WAD in addition to pain, may include greater or more extensive pathophysiological alterations (Kristjansson et al., 2003; Michaelson et al., 2003; Scott et al., 2005). Dizziness, reduced head stability, and reduced accuracy in head repositioning tests may be caused by alteration of the proprioceptive ability (Heikkilä and Wenngren, 1998; Khoshnoodi et al., 2006; Kogler et al., 2000; Michaelson et al., 2003). There may be a higher degree of these disturbances associated with WAD (Michaelson et al., 2003). Eye movement disturbances, and muscle pain may also occur as a result of disorganized neck proprioceptive activity (Gimse et al., 1996; Sterner and Gerdle, 2004).

A reduced activity in the deeper neck musculature, i.e. longus capitis and longus colli, can lead to a greater fatigability of

superficial neck flexor muscles, i.e. sternocleidomastoideus (Falla et al., 2004b; Jull et al., 2004). This altered muscle activation may be more prominent in WAD patients (Falla et al., 2004). In addition, patients with chronic WAD have unnecessarily increased muscle tension which partly can be due to peripheral alterations in the muscles (Elert et al., 2001; Fredin et al., 1997).

In a recent study by Sundström and co-workers, differences in cerebral blood flow indicated different pain mechanisms in patients with non-specific neck pain as compared with WAD patients (Sundström et al., 2006). In addition, microdialysis studies indicate different pain mechanisms between WAD and patients with chronic work-related trapezius myalgia (Gerdle et al., 2008; Rosendal et al., 2004; 2005). In both patient groups, peripheral nociceptive processes seem to be activated and serotonin levels are increased (Rosendal et al 2004; 2005). This may be due to different primary sources of nociception, e.g. from different structures in the cervical spine in WAD patients (Barnsley et al., 1995) and on the contrary from an altered muscle pattern in work-related pain (Rosendal et al., 2005). In addition, WAD patients seem to have a more generalized hypersensitivity (Gerdle et al., 2008; Scott et al., 2005).

3.4 Diagnostic methods

For medical and insurance reasons it is important with an early diagnosis (Carlsson et al., 2005; Miettinen et al., 2004). Routine use of radiographs and MRI are not recommended when examining patients with neck pain, especially since findings of cervical spine injuries are rare (Bonuccelli et al., 1999; Heller et al., 1983; Nidecker et al., 1997; Sweetman, 2006; Taylor and Taylor, 1996). As mentioned, subtle lesions on intervertebral discs cannot be seen on radiographs (Taylor and Taylor, 1996). Question-based decision systems can be used to decrease the number of unnecessary radiographs in patients with suspected spine injuries (Daffner, 2001; Kerr et al., 2005; Stiell et al., 2001). The clinical examination in general includes range-of-movement test of the neck and palpation of neck and shoulder muscles. In many cases with WAD, the only sign is muscle pain in the neck

and shoulders (often after repetitive arm, shoulder and neck movements). Muscle palpation reveals if an increased tenderness is present i.e. lowered pain thresholds for pressure. From a theoretical point of view this can have different origins. It can be primary and/or secondary hyperalgesia (i.e., a generalised increased pain sensation caused by alterations of peripheral or central neurons involved in pain transmission). It can also be a referred pain from facet joints (Barnsley et al., 1995).

Once any signs of potentially serious disease or trauma have been ruled out, the physician or physiotherapist can consider the condition to be non-specific neck pain (Bogduk, 1988; Bogduk and Marsland, 1988; Moffett and McLean, 2006). If the patient was exposed to an accident (such as a rear-end car accident), WAD can be the cause of the neck pain. Since different structures in the neck can be damaged, WAD is heterogeneous and can be considered to be a syndrome. In clinical practice it is still difficult to identify subgroups and thus establish a more precise diagnosis and a more optimized treatment (Sterner and Gerdle, 2004).

Treatments for people with neck pain are, e.g. passive and active physiotherapy, cognitive behavioural interventions, medication and manipulation (Borghouts et al., 1998; Sweetman, 2006). For chronic or long-term neck pain, extensive multidisciplinary or multimodal rehabilitation strategies may be most effective (Carlsson et al., 2005; Sweetman, 2006).

4 Kinematics

Kinematics describes the motion of objects without the consideration of the masses or forces that create the motion. Linear kinematics is the simplest application, while rotational kinematics is more complicated. The state of a rigid body may be described by combining both translational and rotational kinematics (rigid-body kinematics). Human movements are often described with multi-segmental models, consisting of rigid bodies linked together by joints with appropriate degrees of freedom.

A rigid body's movement in space can, on its general form, be described by its rotation and translation relative a global reference system. The rotation is defined by the 3×3 rotation matrix, **R**, while the translation is defined by the 3D translation vector, **v**. Different approaches can be used to decompose **R** and **v** into a physically interpretable description. Most commonly, the relative rotations of body segments are given instead of referring to a global reference system, for example the flexion/extension of the upper arm is given relative to the upper body. The Euler method, where **R** is decomposed into angles describing flexion-extension, abduction-adduction and internal-external rotation is common in clinical applications. The Helical axis method is common when joint translation needs to be included. Then the movement of a segment is described with a rotation angle around, and a scalar translation along, a axis that are allowed to move in space. (Zatsiorsky, 1998)

Other methods are the Matrix method and the Quaternion method (not described here). The quaternion presentation of body movement is at the present point in time not as common within biomechanics, but is for example used to describe sequential eye movements (Tian et al., 2007; Tweed and Vilis, 1990). It is also widely used within robotics science and computer graphics.

4.1 Euler/Cardan method

The Euler transformation has become a golden standard within biomechanics and medicine. Euler angles are easy to interpret. The segment's rotation is described by three angles and the reference system can be aligned with the body segment so that the three angles (α, β and γ) describe flexion-extension, abduction-adduction and inward/outward rotation respectively (Fig. 4.1).

In the Euler convention, the change of orientation is described as a sequence of three successive rotations. Finite rotations are not commutative ($\mathbf{A}^T \cdot \mathbf{B} \neq \mathbf{B}^T \cdot \mathbf{A}$), so different orientation sequences can be used to describe the displacement.

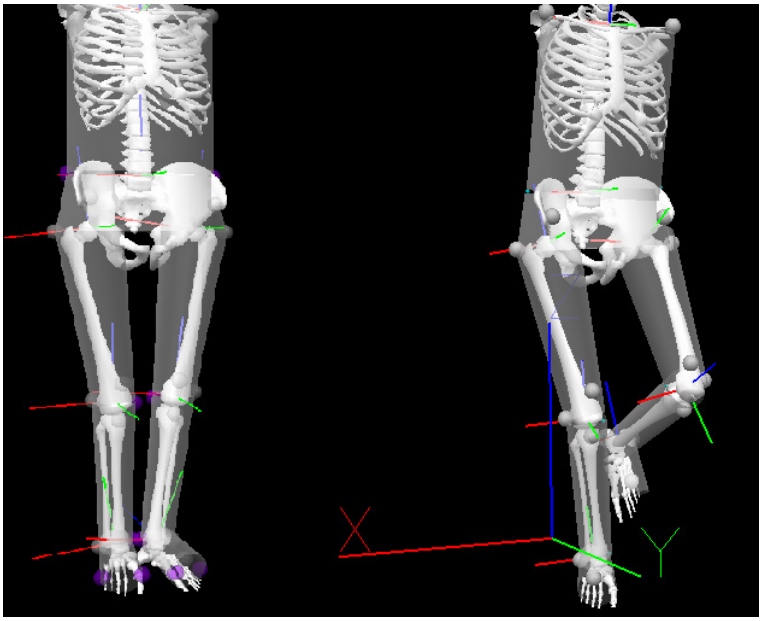

Fig. 4.1. An optical motion capture system and reflective markers (grey circles) have been used to collect motion data. Visual3D software (C-motion, Inc.) was used to visualize body segments. Euler angles can be used to describe knee flexion as rotation around X, abduction/adduction as rotation around Y and inward/outward rotation as rotation around Z.[2]

[2] This figure was generated from Visual3D by the author

A common convention is the Cardan sequence **Zy'x''**; a rotation around **X** followed by a rotation around **Y** followed by a rotation around **Z**. Note that each rotation changes the direction of the initial reference system (which is why different rotation sequences are not commutative). Then **R** is defined as

$$\mathbf{R}(\alpha,\beta,\gamma) = \mathbf{R}(\alpha\mathbf{Z}) \cdot \mathbf{R}(\beta\mathbf{y}') \cdot \mathbf{R}(\gamma\mathbf{x}'')$$

$$\mathbf{R} = \begin{bmatrix} \cos(\alpha) & -\sin(\alpha) & 0 \\ \sin(\alpha) & \cos(\alpha) & 0 \\ 0 & 0 & 1 \end{bmatrix} \cdot \begin{bmatrix} \cos(\beta) & 0 & \sin(\beta) \\ 0 & 1 & 0 \\ -\sin(\beta) & 0 & \cos(\beta) \end{bmatrix} \cdot \begin{bmatrix} 1 & 0 & 0 \\ 0 & \cos(\gamma) & -\sin(\gamma) \\ 0 & \sin(\gamma) & \cos(\gamma) \end{bmatrix}$$

$$\mathbf{R} = \begin{bmatrix} \cos\alpha\cdot\cos\beta & \cos\alpha\cdot\sin\beta\cdot\sin\gamma - \sin\alpha\cdot\cos\gamma & \cos\alpha\cdot\sin\beta\cdot\cos\gamma + \sin\alpha\cdot\sin\gamma \\ \sin\alpha\cdot\cos\beta & \sin\alpha\cdot\sin\beta\cdot\sin\gamma + \cos\alpha\cdot\cos\gamma & \sin\alpha\cdot\sin\beta\cdot\cos\gamma - \cos\alpha\cdot\sin\gamma \\ -\sin\beta & \cos\beta\cdot\sin\gamma & \cos\beta\cdot\cos\gamma \end{bmatrix}$$

The Euler angles is then extracted from **R** as

$$\alpha = \tan^{-1}\left(\frac{R_{21}}{R_{11}}\right)$$

$$\beta = \tan^{-1}\left(-\frac{R_{31}}{\sqrt{{R_{11}}^2 + {R_{21}}^2}}\right)$$

$$\gamma = \tan^{-1}\left(\frac{R_{32}}{R_{33}}\right)$$

Flexion is hence described by γ (rotation around **x**''), abduction/adduction by β (around **y**'), and inward/outward rotation by α (around **Z**). Different conventions give different representation of the angles as illustrated in Fig. 4.2. The rotation matrix **R** is the same, regardless of how you choose to extract the Euler angles from it.

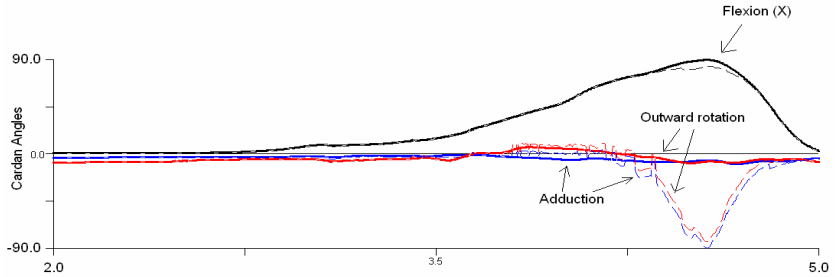

Fig. 4.2. Knee rotation using two different cardan sequences (Xy'z''; thick lines, and Zy'x''; dashed lines). Knee flexion is approximately the same in both conventions. Outward rotation is close to zero in the Xy'z'' convention but close to -90 in Zy'x''. This relates to that angles are periodical, i.e., 0 and -90 describe the same angle. In this case, the Xy'z'' is most appropriate convention to use. [3]

The Euler/Cardan method has some drawbacks. For example, when two or more axis aligns, **R** is not uniquely determined, thus resulting in a singularity, or a "gimbal lock". Therefore you need to orient the local reference systems in order avoid the gimbal lock situations. It is also important to align the reference system with the body segments correctly, so that parts of abduction/adduction and inward/outward rotation are not superimposed in the calculated flexion. Another drawback is that the translation (**v**) has to be handled separately. If you want translation to be included in the model, the helical axis transformation can be used.

4.2 Helical axis method

In three dimensions, the motion of a body from one instance to another can be broken down into a rotation about and a translation along the instantaneous axis of rotation (Fig. 4.3). The helical axis is not fixed in space, but is defined by its unit direction vector, **n**, and a point **c** on this axis fulfilling $\mathbf{c}^T \mathbf{n} = 0$. The rotation is given by the angle of rotation, θ, about the helical axis and the translation is given by a scalar translation, *t*, along it (Spoor and Veldpaus, 1980; Woltring et al., 1985; Woltring et al., 1994). This

[3] This figure was generated from Visual3D by the author

description is called the helical axis method. The helical axis is also known as the screw axis or the axis of motion.

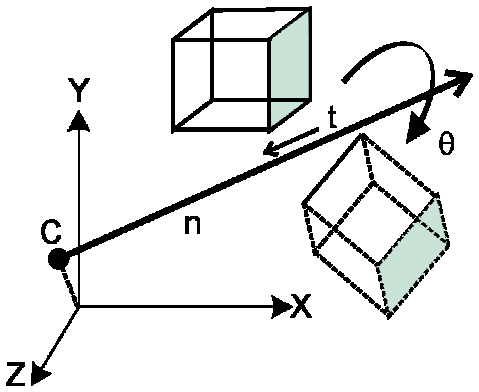

Fig. 4.3. Movement according to the Helical axis method. The rigid body rotates around an instantaneous axis that is allowed to move. The axis position is given by its direction vector **n** and a point **c** on the axis. The slide along the axis is given by the scalar *t*.

The helical axis characteristics is extracted from **R** and **v** by defining a matrix **U** that fulfils $\mathbf{U} = \mathbf{R}^{\mathrm{T}} - \mathbf{R}$ (Söderkvist, 1990). It can be showed that:

$$\mathbf{n} = \frac{1}{\sqrt{U_{23}{}^2 + U_{31}{}^2 + U_{12}{}^2}} \cdot \begin{bmatrix} U_{23} \\ U_{31} \\ U_{12} \end{bmatrix}$$

$$\theta = \begin{cases} \arccos\left(\dfrac{R_{11} + R_{22} + R_{33} - 1}{2}\right) \\ \arcsin\left(\sqrt{U_{23}{}^2 + U_{31}{}^2 + U_{12}{}^2}\right) \end{cases}$$

$$\mathbf{c} = \frac{1 + \cos\theta}{2\sin^2\theta} \cdot \left(\mathbf{I} - \mathbf{R}^{\mathrm{T}}\right)\mathbf{v}$$

$$t = n^T \mathbf{v}$$

The helical axis method is useful when analyzing the joint translations, since the axis is allowed to move in space. This, in turn, gives the possibility to study the actual movement of the centre of a joint by deriving the intersection of at least two instantaneous helical axes from two different points in (centre of rotation, see below).

The drawback is that the error in orientation and location of the helical axis is large for small rotations, since it is inversely proportional to rotational magnitude (Woltring et al., 1985). Another drawback is that a clinical interpretation of the movement (such as amount of flexion) is more difficult to make than when using the Euler representation.

In Paper IV in this dissertation, it is proposed that the intersection of all finite (or instantaneous) axes may be used to define a 3D centre of the axis of rotation, **CR** (Fig. 4.4). It should not be mistaken to be a physical point, like a joint centre. Instead it could be compared to the centre of mass, which can actually lie outside a body. For example, **CR** is not defined for parallel axes, and for axes near to parallel, the **CR** will lie far from the rotating body. During circular movements of a segment around a pivot point, all finite helical axes describing the movement would intersect in the pinot point (e.g approximately in the hip joint when moving the thigh relative to the hip).

Each helical axis can be described by a line $\boldsymbol{l}_i\,(a_i) = [\mathbf{c}_i, \mathbf{c}_i + a_i\mathbf{n}_i]$, where a_i is a scalar and **c** and **n** are 3D vectors. The cervical spine consists of several joints. Due to this, and to measurement errors, the point of intersection may be computed as the solution to the overdetermined least squares problem

$$\min \sum_{i=1}^{n} \left(\mathbf{CR} - \boldsymbol{\ell}(a_i)\right)^2$$

where n is the number of helical axes.

On matrix form, this becomes

$$\min \left\| \begin{bmatrix} \mathbf{n}_1 & & & & \mathbf{I} \\ & \mathbf{n}_2 & & & \mathbf{I} \\ & & \mathbf{n}_3 & & \mathbf{I} \\ & & & \ddots & \mathbf{I} \\ & & & \mathbf{n}_n & \mathbf{I} \end{bmatrix} \bullet \begin{bmatrix} a_1 \\ \vdots \\ a_n \\ CR_x \\ CR_y \\ CR_z \end{bmatrix} - \begin{bmatrix} \mathbf{c}_1 \\ \mathbf{c}_2 \\ \vdots \\ \mathbf{c}_n \end{bmatrix} \right\|$$

where **I** is the 3×3 identity matrix. By using QR-decomposition, **CR** can be computed (Golub and van Loan, 1983).

The condition number can also be used to describe the parallelism of the axes. It is defined as the ratio of the largest singular value of the matrix of vectors to the smallest singular value. It therefore approaches infinity if the matrix contains completely parallel vectors, and approaches 1 for vectors that are close to perpendicular.

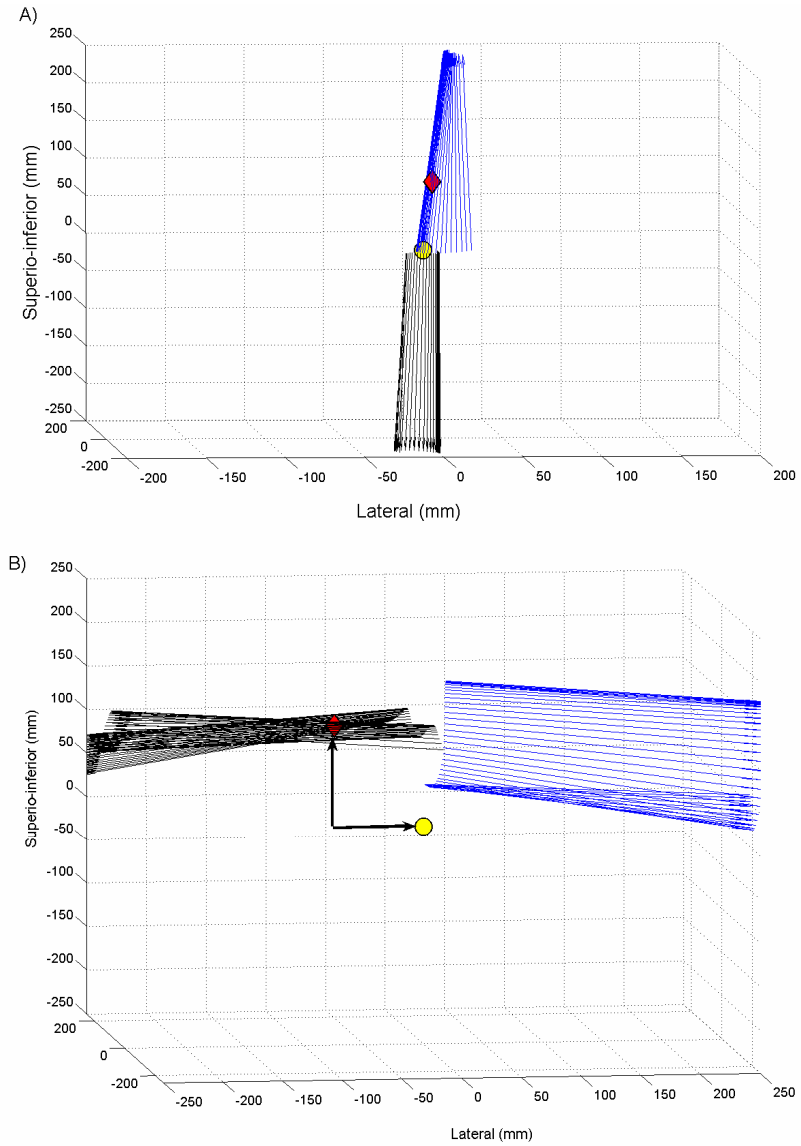

Fig. 4.4. The intersection of the axes can be used to define a 3D centre of the helical axes, **CR** (red square). The yellow point is the reference point (0,0,0). In A), **CR** is derived by combining axes from right (black lines) and left side rotations (blue lines). In B), **CR** is derived by combining axes from flexion (black lines) and extension (blue lines). The vectors in B) show the lateral and sagittal components of **CR**.

4.2.1 Instantaneous and finite approaches

For slow movements or short displacements, instantaneous helical axes can be approximated with finite helical axes as described above. For high-speed data, position and direction of instantaneous helical axes may be calculated by using the velocity vectors and matrices (Woltring et al., 1985). The angular velocity matrix and vector (**W** and **w**) for two adjacent time frames ($\Delta t = t_i - t_{i-1}$) are defined as

$$\mathbf{W} = \dot{\mathbf{R}}\mathbf{R}^{T} \approx \frac{1}{4\Delta t}\left(\mathbf{R}_i\mathbf{R}_{i-1}^{T}\right)$$

$$\mathbf{w} = \begin{pmatrix} W_{32} - W_{23} \\ W_{13} - W_{31} \\ W_{21} - W_{12} \end{pmatrix}^{T}$$

Then, helical axis position and direction can be solved as.

$$\mathbf{n} = \frac{\mathbf{w}}{\|\mathbf{w}\|}$$

$$\mathbf{c} = \bar{\mathbf{x}} + \frac{\mathbf{W}d\bar{\mathbf{x}}/dt}{\|\mathbf{w}\|^2}$$

, where $\bar{\mathbf{x}}$ is the mean position of the marker cluster or motion sensor and ||**w**|| is the magnitude of the angular velocity.

5 Movement analysis systems

Movement of the cervical spine is difficult to investigate accurately and non-invasively because of its complex anatomic structure and compensatory movements (for example from visual and vestibular information). The choice of analysis method primarily depends on the examiner's goal. If the goal is a clinical screening, certain types of goniometers, e.g. Myrin devices (Malmstrom et al., 2003; Mellin, 1986), show good reproducibility and reliability in evaluating maximal cervical ROM. Routine use of radiographs are not recommended since findings are rare and to avoid excessive X-ray exposure (Heller et al., 1983; Sweetman, 2006). If the goal is a thorough investigation and follow-up of neck function for post-traumatic cervical spine disorders, kinematic analysis with optical motion capture systems are reliable and reproducible methods (Antonaci et al., 2000; Wong et al., 2007). A drawback is that these systems are expensive and time-consuming and they require special laboratory environments and special training of the personnel (Antonaci et al., 2000; Wong et al., 2007). A new promising method is sensor systems based on miniaturized accelerometers and gyroscopes. The small size and weight of those components makes it possible to mount them on body segments to track body motion. This technique can turn out to be appropriate for clinical measurements since the devices are small and accurate (Jasiewicz et al., 2007), and may be used in a more natural setting than a movement analysis laboratory. Disadvantage is that appropriate filtering of the data is required due to drift in the signals, and that calculations of position may be less accurate than e.g. optical systems (Giansanti et al., 2003; Wong et al., 2007).

5.1 Optical motion capture systems

A typical optical system consists of at least two video cameras, together with a set of markers. Typically, infrared (IR) cameras together with retro-reflective markers are used (such as ProReflex; Qualisys AB and Vicon motion systems; Vicon AB). The system consists of either active or passive markers. In a system with passive markers, IR light is sent from each camera with a certain pulse frequency. The light is reflected by markers attached on the body segments, and a 2D representation of the markers is captured by each camera (Fig. 5.1). A calibration procedure is done to transform the 2D data from each camera into 3D co-ordinate data. When using active markers, the markers emit a signal, e.g of IR light. Each marker has its own specific frequency, and can easily be identified during the movement registration. (Nigg et al., 2003)

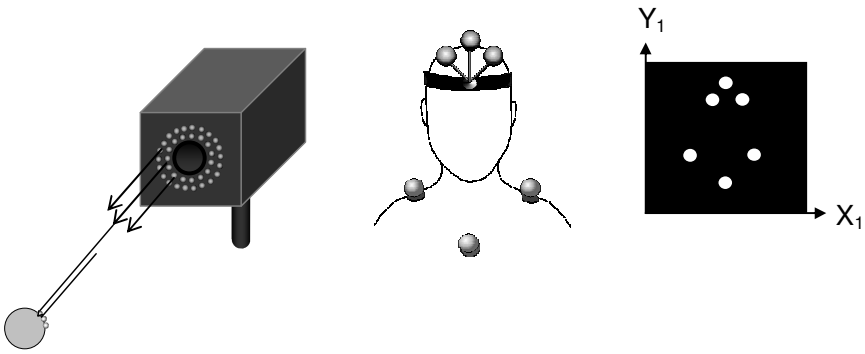

Figure 5.1. Movement registration using IR-cameras and retro-reflective markers. The IR light is reflected from the marker back into the camera, where a 2D image of the markers is registered.

The markers are either placed on anatomical positions (as in Fig. 4.1) or to define local reference systems for each segment and calculate relative rotation angles (2D or 3D). There can be difficulties with skin movement and momentarily hidden markers. To avoid this, one can use rigid clusters of markers (as in Fig. 5.1) to construct **R** and **v** for the segments movements, and then calculate angles and/or translations.

5.2 Finding R and v from skin markers

As described in Chapter 4, a rigid body's movement in space is described by its rotation **R** and translation **v** relative a global reference system. Söderkvist and Wedin introduced a refinement of the method by Spoor and Veldpaus to construct **R** and **v** for a body segment from a set of skin markers (Spoor and Veldpaus, 1980; Söderkvist and Wedin, 1993). This method requires co-ordinates from at least three markers distributed on the body segment.

If $\mathbf{a_1}, \mathbf{a_2}, \ldots, \mathbf{a_n}$ are the position vectors of each marker at time t_1 and $\mathbf{b_1}, \mathbf{b_2}, \ldots \mathbf{b_n}$ are the position vectors at time t_2, this equation describes the movement between the two points in time:

$$\mathbf{0} = \sum_{i=1}^{n} \left\| \mathbf{b}_i - \mathbf{R}\mathbf{a}_i - \mathbf{v} \right\|, \; n = \text{number of markers}$$

This equation cannot be solved exactly. Firstly, there are always errors in the measured marker positions, $\mathbf{p_i}$. Secondly, the relative positions within the marker group may vary during movement. Since body segments are not completely rigid, and if non-rigid clusters are used, the skin may slide against the bone. The expression instead has to be minimised:

$$\min_{R,v} \sum_{i=1}^{n} \left(\left\| \mathbf{p}_i - \mathbf{R}\mathbf{a}_i - \mathbf{v} \right\| \right)^2$$

This can be done in a number of ways. For example, Söderkvist and Wedin use singular value decomposition (See Appendix) to determine which **R** and **v** that minimise the equation. **R** and **v** are decomposed into rotation angles and/or position by an appropriate convention (See Chapter 4).

5.3 Motion sensor systems

Miniaturized accelerometers that register linear accelerations, and/or angular rate gyroscopes that register angular velocity, can be mounted on body segments to register movement.

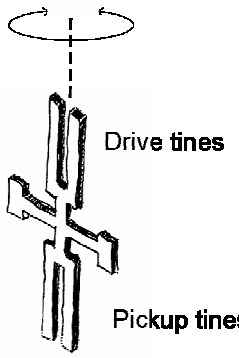

Fig. 5.2. A miniaturized angular gyroscope

An accelerometer can be constructed from a small mass mounted on a base which is in contact with a piezoelectric component. When a varying motion is applied to the accelerometer, the crystal experiences a force from the mass that cause a proportional electric charge that can be measured as an electric signal (Eren, 1999). An angular rate gyroscope consists of a spinning mass (often a disc or a wheel), which is mounted on a base so that its axis can move freely. Thereby the gyroscope's direction is maintained regardless of the movement of the base. An example of a gyroscope in the form of a vibrating tuning quartz fork is shown in Fig. 5.2. The drive tines are driven by an oscillator circuit at a precise amplitude, and oscillates in opposite directions at a rate W_i. When the gyroscope rotates at an instantaneous angular rate of V_r, a Coriolis force acts on each tine ($2mW_i \times V_r$), creating a resulting torque. The tourque in its turn causes the pickup tines to move in and out of the plane, producing an output voltage proportional to the angular rate (Pinney and Baker, 1999).

Coley used gyroscopes to detect gait parameters such as "toe-off" and "heel-strike" (Coley et al., 2005). Combinations of accelerometers and gyroscopes have been used to measure angular rotations of knee and lower limb (Favre et al., 2008;

Mayagoitia et al., 2002). Zhou used a combination of a tri-axial accelerometer, a tri-axial gyroscope and a tri-axial magnetometer to determine the translation and rotation of the wrist and shoulder joint (Zhou et al., 2008). Euler angles and translation of wrist and shoulder joints were derived by an integration process, with angular errors below 5°, and position errors less than 1 cm.

5.4 Electro-oculography

Head and neck movement is influenced by visual information. Combined measurements of head and eye movement can be done in order to study eye and head co-ordination. One method for eye movement registration commonly used for different clinical applications is electro-oculography, EOG (Brown et al., 2006). EOG measures the corneo-retinal potential of the eye. Since the cornea has a positive potential as compared to the retina, the measured surface potential changes as the eyes rotate (Fig. 5.3).

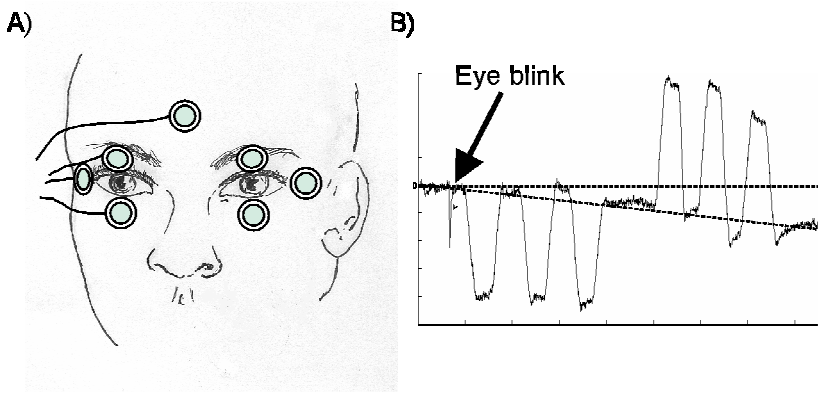

Fig. 5.3 Placement of electrodes for eye movement measurements with electro-oculography (A). Horizontal eye movements are measured by electrodes on the side of each eye, while vertical movements are measured with electrodes above and under each eye. A ground electrode is placed at the forehead as a reference. The signal (B) illustrates EOG output from left and right eye rotations. An eye blink gives a characteristic peak in the EOG signal. Signal drift causes a decrease of the baseline signal as seen in Fig. 5.3.

Slow eye movements (below 6 Hz) are of interest when studying the vestibulo-ocular reflex[4]. To track fast eye movements (saccades), a higher sampling frequency is needed. The major disadvantage of the electro-oculographic method is the slow DC drift (Schlag et al., 1983) seen in Fig. 5.3.B. This drift can be compensated for with a linear fit or with a high-pass filter. A frequent calibration of the signal is also needed. Illumination changes the corneo-retinal potential, and therefore a constant light is required during measurements (North, 1965). Artifacts from eye blinking (Fig. 5.2) and other electrical signals (mainly from muscle activity) also have to be taken into consideration. However, because of its simplicity and convenience, the EOG method is widely used (Alanko, 1984; Brown et al., 2006; Ingster-Moati et al., 2007; North, 1965; Schlag et al., 1983).

[4] To keep the gaze fixed on a non-moving object, the eye counter-rotates in the opposite direction from the head movement.

6 Pattern classification

Pattern recognition that is done with ease in daily life, such as identifying the shape of an object or recognizing a face, is carried out by complex neural and cognitional processes. Technical systems and classification algorithms for automatic pattern recognition have been developed and are widely used, e.g. within speech recognition and DNA sequence identification. There are different approaches to pattern classification depending on the type of problem that should be solved and the amount of data that is to be analyzed. In this chapter, two different classification methods useful for medical applications are described: artificial neural networks and partial least squares regression.

6.1 Artificial neural networks

Artificial neural networks (ANN) were introduced in 1943 when McCulloch and Pitts presented a simplified model of a brain cell (neuron), to understand how neurons can produce highly complex patterns when connected together (McColough and Pitts, 1943). Each neuron was modelled as a threshold logic unit that could perform simple, boolean functions, and several units connected together could solve any logical problems. In 1958, Rosenblatt introduced the perceptron model, composed of in- and output layers of neurons or "nodes" (Rosenblatt, 1958). All nodes were connected and assigned to each connection was a "weight" which could be adjusted (trained) so that the associated connections produced a desired output for a given set of inputs. The neural network models could not solve nonlinear problems until 1983, when John Hopfield added feedback connections to the network, and showed that with these connections the network was capable of "memory", i.e. it had the ability to reconstruct a corrupted

pattern (Hopfield, 1982). Together with the re-discovery[5] of the backpropagation algorithm (Rumelhart et al., 1986), this lay the foundation for multilayer feedforward back propagation neural networks (BPNN), used for different classification problems.

6.1.1 Resilient backpropagation neural network

The BPNN structure consisted of an input layer, one or more hidden layers and an output layer (Fig. 6.1).

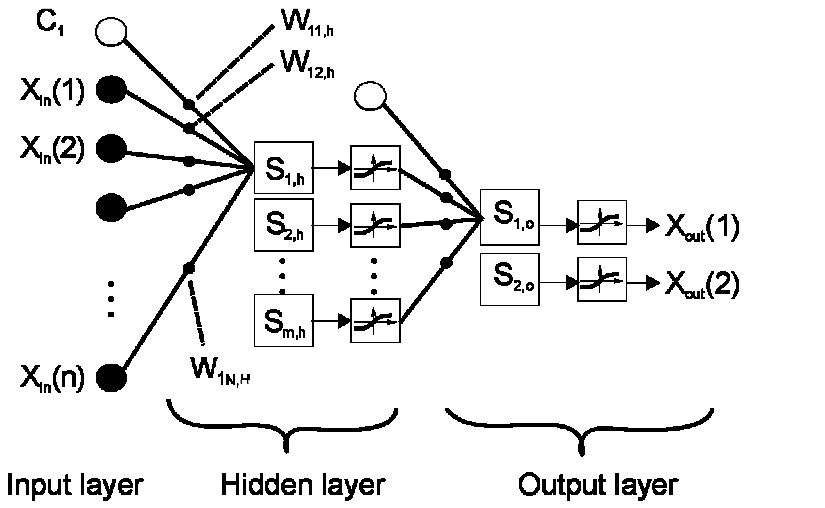

Fig. 6.1. A BPNN network, consisting of an *n*-dimensional input layer, a hidden layer with *m* nodes and a 2D output layer. Each node is connected to the previous layer with weights, w_{jk}, that are adjusted during a number of training sessions to optimize the relation between $\mathbf{x}_{in}$ and $\mathbf{x}_{out}$. The weighted signal S_k to each node is scaled with a transfer function before it is forwarded to the nodes in next layer.

Each node in the layer is associated with a weight that re-scales the input. The k^{th} node in a hidden layer thus receives a weighted input signal S_k from *n* nodes in the previous layer:

[5] The algorithm had been discussed in two different dissertation twenty years earlier

$$S_k = \sum_{j=1}^{n} w_{jk} \cdot x_j(n) + c_k(n)$$

where c_k is a constant, w_{jk} is the j^{th} weight and x_j is the input from the j^{th} node in previous layer.
The output signal is transformed with a transfer function, before forwarded to all nodes in the next layer. Usually the transfer function give an output between 0 and 1 or -1 and +1, e.g. the hyperbolic tangent function $F_k = \sinh(S_k)/\tanh(S_k)$.

The signals propagate through the network and are finally recalculated into one or more output signals.

6.1.2 Number of hidden neurons

The number of free parameters,i.e. nodes, in the network should not exceed the number of observations, since this may result in an overestimating network (Fig. 6.2). For n_i nodes in the input layer, n_h hidden nodes and n_o output nodes and N observations, the upper limit for free parameters is given by

$$n_h\,(n_i + 1 + n_o) + n_o \leq N.$$

Often, "trial and error" is used to decide the exact number of hidden nodes in the network model.

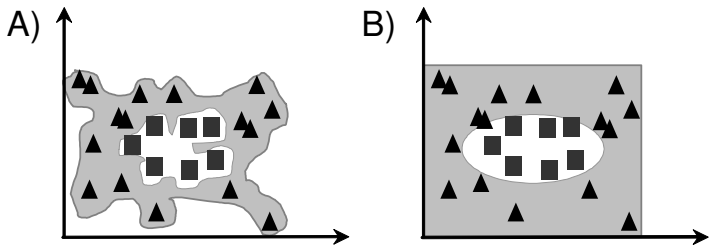

Fig. 6.2. An example of 2D data divided in two classes (white and gray fields) by a neural network. The data points are illustrated as squares and triangles. In A) too many hidden nodes are used, giving a neural network that overestimates the data and a low level of generalisation. In B) the number of hidden neurons is adapted to the degree of difficulty of the data, giving a model with an appropriate generalisation level.

6.1.3 Supervised learning with backpropagation

Unsupervised training categorizes data into a desired number of classes. Vectors with similar "patterns" are grouped together. In supervised training, a set of input vectors with known output, are used to train the network with a chosen algorithm. The goal is then to adjust the weights in order to optimize the relation between input and output signals. In each training session, the error gradients of each weight, $\partial E_p/\partial w_{jk}$, and training vector are calculated. The weights are then adjusted in the direction of this error gradient. As the name indicates, the error is adjusted by backward propagation, i.e. layer by layer. The training continues until a predefined error threshold is reached. To avoid an overestimating network model (Fig. 6.2B), a validation set can be used. The output errors of the test and training group are calculated, and the training terminates when the error in the validation set exceeds the error in the training set.

6.2 Partial least squares regression

Partial least squares regression, PLS, is often used to extract relevant information from a large amount of data, i.e. when the number of subjects or observations, *n*, is smaller or equal to the number of measured variables, *m*. It is an extension of multiple linear regression. The linear multiple regression model describes the linear relationship between a set of dependent variables, **Y** and a set of *m* predictor variables, **X**:

$$\mathbf{Y} = \beta_0 + \beta_1 x_1 + ... + \beta_m x_m + \mathbf{E}$$

where β is a constant and **E** is the error residual. Multiple linear regression works best if **X** is orthogonal (the predictors are linearly independent) – which is seldom the case.

In PLS, both predictors and dependent variables are transformed into new, linearly independent variables prior to linear regression using principal component analysis, PCA (see Appendix 2). This makes it possible to concentrate the information hidden in noisy and possibly redundant **X** and **Y,** and find relationships between

the transformed $\hat{\mathbf{X}}$ and $\hat{\mathbf{Y}}$ variables. While PCA is a maximum variance projection of **X**, PLS is a maximum covariance model of the relationship between **X** and **Y** (Eriksson, 1999).

6.2.1 Exctracting new variables

Supose that **X** is a m×n matrix of *m* predictors and *n* observations, and **y** is a 1×n vector of one dependent variable and *n* observations. The first step is to remove the mean and scale **X** to unit variance ($\bar{\mathbf{X}}$), in order to weight all predictors equally. The next step is to find a vector, $\mathbf{t}_1$, in **X** space that is well fitted to the observations (6.3.A) and correlates to **y**, i.e. $c_1\mathbf{t}_1 = \hat{\mathbf{y}}_1$. (6.3.B).

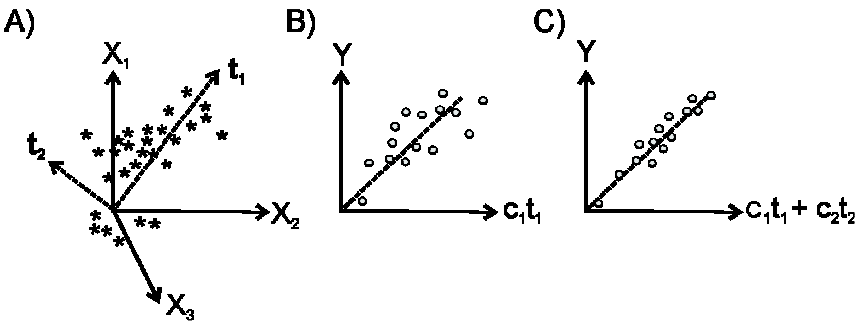

Fig. 6.3 A-C. Transformation of **X** and **y** into new linearly independent variables. A) shows the extraction of the two first principal components. B) shows the correlation between the first component and **y**, and C) shows the correlation between linear combinations of the two principal components.

The variance that could not be explained by $\mathbf{t}_1$ is described by the residuals $\mathbf{f}_1 = \mathbf{y} - \hat{\mathbf{y}}_1$ (Fig 6.3.B). Additional components $\mathbf{t}_2$, $\mathbf{t}_3$, etc. may be computed to take the unexplained variance into account. The second component is orthogonal to $\mathbf{t}_1$ (Fig. 6.3.A). If $\hat{\mathbf{y}} = c_1\mathbf{t}_1 + c_2\mathbf{t}_2$ is better correlated to **y** than $c_1\mathbf{t}_1$ (Fig. 6.3.C), this model is considered as better. The final model for **X** is:

$$\mathbf{X} = \mathbf{I}\bar{\mathbf{X}} + \mathbf{T}\mathbf{P}^{T} + \mathbf{E}_{X}$$

where **I** is the identity matrix, **T** contains the significant principal components (i.e. transformed x variables), **P** is a weight matrix with variable loadings and $\mathbf{E}_X$ contains the remaining unexplained variance in **X**. In the same way, the final model for transformed dependent variable(s) is:

$$\mathbf{Y} = \mathbf{I}\bar{\mathbf{Y}} + \mathbf{U}\mathbf{C}^{T} + \mathbf{E}_{Y} = \mathbf{I}\bar{\mathbf{Y}} + \mathbf{T}\mathbf{C}^{T} + \mathbf{E}^{*}$$

where, **U** contains the transformed y variables **C** is the weight matrix and $\mathbf{E}_Y$ is the remaining unexplained variance in **Y** (or **y**).

The transformed predictor variables ($\mathbf{t}_1$, $\mathbf{t}_2$,…) may be plotted to illustrate sub groups, outliers and trends. The variable loadings of **P** are listed, to show how much each originally predictor variable $\mathbf{x}_i$ contribute to each significant principal component $\mathbf{t}_a$. Variable influence on projection (VIP) describes the relevance for each $\mathbf{x}_i$ to predict **y**. VIP is received by summing all weights between the predictor $\mathbf{x}_i$ and significant principal components $\mathbf{t}_a$:

6.2.2 PLS regression

In the PLS regression, a linear relationship is found between **y** and **X** such that **y** = f(**X**) + **E**, where f(**X**) is a polynomial function of the transformed predictor variables:

$$\mathbf{VIP_i} = \sum_{a=1}^{k} (w_{a,i})^2 \cdot R^2_{a,x}$$

where $k < m$ = number of significant $\mathbf{t}_a$ and $R^2_{a,x}$ is the variance in X explained by $\mathbf{t}_a$. (Eriksson, 1999).

7 Aims

The general aims were:

1) To further develop objective biomechanical methods and models to analyse head and neck movement, with focus on subjects with neck pain.

2) To investigate whether individuals with WAD show more severe disturbances than individuals with non-specific neck pain as compared with asymptomatic controls.

3) To investigate whether analyses of head and neck movements have the potential as a decision support for physicians and physiotherapists during diagnosis and follow-up of neck pain patients.

8 Review of included papers

8.1 Paper I

Head kinematics was studied within two groups: one consisting of 59 subjects with WAD and one consisting of 56 controls, CON. 3D motion data were collected during fast repetitive head movements (flexion, extension, right and left side rotation) using an optical motion capture system and rigid marker clusters. Head rotation relative to the upper body was derived with the Helical axis method, and head movement variables such as mean and maximum angular velocity, range of movement (ROM), symmetry of movement (left as compared with right, flexion as compared with extension) were calculated. A partial least squares regression (PLS) discriminant analysis predicted group membership with a predictive power of 61% (R^2=0.63, Q^2=0.61). Maximum and mean angular velocity were most important when discriminating between the WAD and CON groups, even though differences were found in several movement variables. (Öhberg et al., 2003)

8.2 Paper II

A back propagation neural network, BPNN, was trained with neck movement variables from the same subjects as in Paper I. A principal component analysis was first performed in order to reduce data and improve the BPNN performance and an optimal BPNN structure was then constructed. Each subject was classified by the trained network according to group membership by the leave-one-out method. BPNNs with six hidden nodes had a predictive ability of 0.89, with sensitivity (i.e. correct classified WAD subjects) of 0.90 and specificity (i.e. correct classified CON subjects). of 0.88 (Grip et al., 2003)

8.3 Paper III

The repositioning error and irregularities in position (**c**) and direction (**n**) of the helical axis ("axis of motion") were analyzed during a head repositioning task within a group of 24 controls, a group of 22 individuals with WAD and a group of 21 individuals with non-specific neck pain (NP). The head rotation angle, θ, was derived in the same way as in Papers I-II. The constant, absolute and variable repositioning errors were calculated. The finite helical axis position and direction were calculated for each time frame using a variable time window with a cut-off of $\Delta\theta = 4°$. The 3D angle, ω, between the direction vectors of the mean axis and each finite axis were derived. Variations in the helical axis were estimated by its total trajectory and the standard deviation of ω. Tendencies to increased variation in the WAD group were found, with a significant larger axis trajectory during side rotation to the left. In addition, the WAD group had a larger constant repositioning error during flexion. This indicated disturbances in the sensorimotor control in the WAD group, e.g. in proprioception. The mean position of the axis was about 2 cm lower in both neck pain groups as compared with the CON group during flexion, indicating a change in movement strategy during head bending. Since pain intensity showed an effect on the axis position, this may be the reason for this change in strategy. (Grip et al., 2007)

8.4 Paper IV

The same groups of subjects as in Paper III performed fast repetitive head movements (same protocol as in Paper I-II) and a ball catching task. Helical axis parameters were derived in the same way as in Paper III. In addition, the centre of rotation of the axis was derived by calculating the intersection point of the finite axes, **CR**. Irregularities in **n** and **c** curves were derived with the zero-crossing rate, since the variability measures used in Paper III were not appropriate for ROM movements. A downward shift of **c** and **CR** during flexion/extension and a change of axis direction towards the end of the movement were observed in the control group. **CR** was different during different conditions, with the

most superior position occurring during side rotations and the most inferior during ball catching. One explanation could be that side rotation mainly is done in the upper spine (C1/C2), while all cervical vertebrae are recruited to balance the head during upper body movements as in the catching task. A lower position of **CR** was observed in the CON group as compared with the WAD group during side rotations. This could relate to the fact that the lower cervical spine was recruited to a smaller extent in the WAD group. Rotation of head and upper body was significantly smaller and upper body movement was slower in the WAD group as compared with both the NP and the CON groups even though catching frequency was similar in all three groups. This indicates a stiffer body position in the WAD group during the catching task.. This together with higher zero crossing rates during all performed tasks indicated deficiencies in motor control in the WAD group. (Grip et al., 2008a, *Submitted*)

8.5 Paper V

In this study the reliability of a measurement method based on combined recordings of head and eye kinematics was evaluated. Gaze fixation and head-eye co-ordination were studied using wireless motion sensors and electro-oculography. Twenty asymptomatic control subjects and six subjects with chronic whiplash were included. In the CON group, velocity gain (ratio of eye and head velocities) was close to unity as expected and head stability was high during head-eye coordination. Range of movement during gaze fixation was about 40°, which is close to the natural visual range. The trial-to-trial repeatability was moderate to high (intraclass correlation coefficients 0.4 to 0.9), with some exceptions during head-eye co-ordination. Case studies of whiplash subjects demonstrated decreased head velocity, decreased range of head movement during gaze fixation and a less stable head position during head-eye co-ordination as possible deficits. (Grip et al., 2008b, *Submitted*)

8.6 Summary of the author's responsibility

Table 8.1. Contributions of the author to each paper included in this dissertation

The author's responsibility:	I	II	III	IV	V
Idea and study design	C	B	A	A	B
Planning of the study	B	A	A	A	A
Realisation of the study	A	A	A	A	B
Analysis and summary of results	B	A	A	A	A
Manuscript compilation	B	A	A	A	A
Journal correspondence	B	A	A	A	A

A: main responsibility
B: contributed to a high extent
C: contributed

9 Materials and methods

Ethical approval was obtained from the institutional ethics committee (Papers I-IV: Umeå University, Umeå, Sweden and Paper V: The University of Queensland, Brisbane 4072, Australia). Informed consent was obtained from each subject prior to participating. All procedures were conducted according to the Declaration of Helsinki.

9.1 Subjects

Three subject materials were collected for the studies (in total, 100 control subjects, 87 subjects with WAD and 21 subjects with non-specific neck pain), Table 9.1.

Table 9.1. Summary of subjects that participated in the studies.

Paper	Matched controls	Non-specific neck pain subjects	WAD subjects
I-II	56 (27 F, 29 M) 40 ± 11 yr	Not studied	59 (30 F, 29 M) 38 ± 11 yr
III-IV	24 (16 F, 8 M), 50 ± 18 yr	21 (14 F, 7 M) 49 ±16 yr	22 (5 M, 17 F) 49 ±15 yr
V	20 (9 F, 11 M) 32 ± 9 yr	Not studied	6 (4 F, 2 M) 28 ± 7yr

The controls in Papers I-IV were mainly recruited through advertisements at the University Hospitals in Umeå and Linköping, Sweden, while students and personnel working at the University of Queensland, Brisbane, participated in Paper V. Occasional neck or back pain was accepted as long as subjects hade been free from symptoms during the previous three months.

All individuals with WAD had symptoms lasting longer than three months. The WAD subjects in Papers I-II had received their diagnoses from a physician who had daily experience in the

diagnosis and management of WAD patients. The subjects had different grades of WAD, assigned according to the definitions by the QTF. Subjects in Papers III-IV were recruited via physiotherapists at rehabilitation clinics and medical centres. They had their diagnosis made by physicians at different points in time prior to the study, and were classified as grade 1-2 according to the QTF. The WAD subjects in Paper V had visual complaints and were recruited from patients who attended the university whiplash research unit and via advertising in the local newspaper. They were excluded if they had previously diagnosed vestibular dysfunction and or any associated diseases, vascular risk factors such as low or high blood pressure, migraine, known arteriosclerotic disease or past history of visual problems or dizziness prior to the injury.

9.2 Measurement protocols

Questionnaires rating pain, disability, pain intensity and vision problems were collected. NPAD, DRI and NDI indices are commonly used to describe self-reported neck pain and disability (Salen et al., 1994; Vernon and Mior, 1991; Wheeler et al., 1999). Visual Analog scales (VAS) describe self-reported pain intensity (Carlsson, 1983). EQ-VAS indicates health status (Rabin and de Charro, 2001) and FABQ indicates the subjects fear avoidance beliefs (Waddell et al., 1992). The Vision symptom index (VSI) was constructed and used to rate the frequency and severity of 15 symptoms related to vision such as dizziness, double vision, blurred vision, red eyes, itchy eyes and headache (Study V).

Table 9.2. Questionnaires reporting pain intensity, fear avoidance and disability

Questionnaires	Paper
NPAD: neck pain and disability in everyday life	III-IV
VAS: pain intensity head and neck	
EQ-VAS: perceived health status	
DRI: ability to perform mainly physical daily activities	
FABQ: fear avoidance beliefs	
NDI: neck pain and disability in everyday life	V
VSI: vision problems	

Five different movement conditions were studied:

1) Fast, repetitive head movements (Papers I-II and IV). In total, 20 movements were performed in an order unknown to the subject, including flexion, extension and side rotations to left and right. A board with arrows was placed in front of the subject to direct head movements. A signal was given by illuminating one of the arrows. The subject was instructed to move the head as fast and far as possible without pain as soon as, and in the direction of, the arrow that was illuminated. The control signal to the board was synchronized with the motion analysis system and sampled in order to measure the reaction time.

2) Slow repositioning head movements with closed eyes, from an extended position back to a neutral position (Paper III). After a short training, 20 movements were performed in an order unknown to the subject, including 25° flexion, 25° extension, 30° side rotation to left and 30° to the right. The same board as in **1)** was used to guide the subject. A small electric torch attached to the subject's helmet shone onto the board and guided the subject's head movement to the centre dot of each square. After each performed movement, the subject opened both eyes and actively adjusted the head.

3) Head and upper body movements during ball catching (Paper IV). An arrangement of two tubes was used to roll balls that passed on either the right or the left side of the subject. After 10 training trials for each side, the subject tried to catch 10 balls, rolled in an order unknown to the subject.

4) Gaze fixation (Paper V). The subject kept the gaze fixed on a centre point and then rotated the head as far as possible without loosing gaze fixation.

5) Head-eye co-ordination (Paper V). The subject moved the eyes to the 30° position while holding the head still, then rotated the head to the 30° position while gaze remain fixed. The subject then moved the eyes back to the centre point while head remained in

the 30° position. Finally, the head was rotated back to the neutral position while the gaze was kept fixed.

9.3 Movement registration

In Papers I-IV, movement registration was done with a ProReflex system (Qualisys Medical AB, Gothenburg, Sweden). The system consists of retro-reflective markers, software (QTrac) and cameras emitting and detecting IR light. Four cameras at 60 Hz (Papers I-II) or five at 120 Hz (Papers III-IV) measured light reflected from the markers and computed 2D co-ordinate data for each marker centre. QTrac software was used to construct 3D marker co-ordinates, identify markers and interpolate if any markers were momentarily hidden in the data set. In Papers I-II, two rigid marker clusters (three markers per cluster) were mounted on the subject: one on a fixed frame and one on the torso using an ortho-plastic vest (Fig. 9.1.A). In Papers III-IV, the head marker cluster was increased to five markers. A plate with a cluster of three markers was placed on the back and plates with clusters of four markers were mounted on the upper arms. Markers were also placed on each acromium and on each mandibular fossa as references for calculating cervical length and on the suprasternal notch as a reference for helical axis position (Fig. 9.1.B). In Paper V, two wireless motion sensors (Inertiacube3, Intersense, Inc.,Bedford, MA,USA), placed on C7 and on the forehead, were used to collect head movement data. Synchronized measurements of horizontal eye movement were recorded with EOG, using Ag/AGCl surface electrodes and a powerlab unit 8/SP (ADInstruments, NSW, Australia) Fig 9.1.C. Collection frequency was 50 Hz.

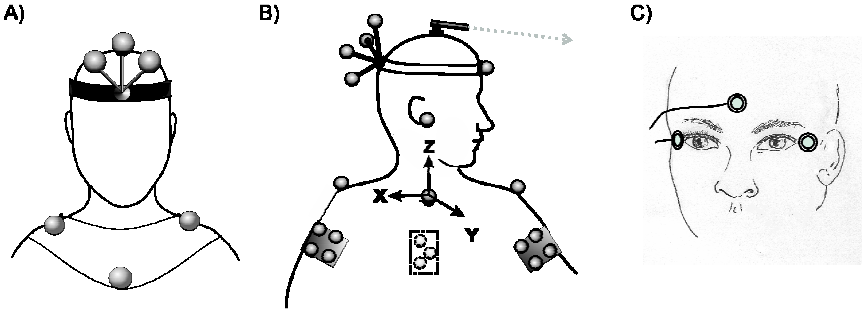

Fig. 9.1. Marker setups in A) Paper I-II and B) Paper III-IV. In C), electrode placement for registration of eye movement are illustrated.

9.4 Kinematical models

All kinematical calculations were done with MATLAB software (Mathworks Inc., Natick MA, version 7.1). In Papers I-IV, angle of rotation, θ, of head and upper arms relative to upper body were calculated using a finite helical axis model (Spoor and Veldpaus, 1980). In Papers I-II, a cubic smoothing spline algorithm was performed on the helical angle, to permit calculation of the time derivative. In Papers III-IV, the raw coordinate data were filtered with a low-pass Butterworth filter (2^{nd} order) using a cut-off frequency at 6 Hz before further calculations.

Finite position, **c**, and direction, **n**, of the helical axis were approximated by using a floating time window with a cut-off set to $\theta = 4°$, and filtered once more with the same filter. A marker placed on the suprasternal notch was used as a reference point for helical axis position for all calculations. The 3D angle, ω, between each finite axis direction vector and the mean direction vector was derived. In Paper IV, the intersection of the axes was used to define a finite centre of rotation for the total range of movement and for consecutive 15-degree-intervals of the movement. In addition the condition number was calculated as a measure of diversity among the helical axis direction vectors. Variations in the helical axis were estimated by its total trajectory and the standard deviation of ω (Paper III) or by the zero crossing rate in **n** and **c** (Paper IV).

In Paper III; the absolute head repositioning error was estimated by the helical angular displacement. The major axis Euler angles were used to calculate constant and variable errors, since the helical angle by definition is ≥ 0 and could not be used directly. This gave:

$$\text{Absolute error} = \frac{\sum_{j=1}^{n} \Theta_j}{n}, \quad n = 5$$

$$\text{Constant error (CE)} = \frac{\sum_{j=1}^{n} \phi_{euler,j}}{n}, \quad \phi_{\text{euler}} = \begin{cases} \alpha, \text{ flexion/extension} \\ \gamma, \text{ axial rotation} \end{cases}$$

$$\text{Variable Error} = \sqrt{\frac{\sum_{j=1}^{n} \left(\phi_{euler,j} - CE\right)^2}{n}}$$

In Paper V, head rotation relative to space and eye rotation relative to head were studied, and the Euler angle in the primary plane defines side rotation of the head. EOG was used to describe the rotation angle of the eyes. The EOG and head angle data were filtered using a 3rd order Butterworth low-pass filter with a cut-off frequency of 5 Hz, and a linear fit was used to reduce effects from linear drift. Initial position was set to 0° for both the head and eye prior to each new repetition. The EOG data were normalized to angular rotation, using reference measurements of 30° left and right eye rotations. Blinking was identified and replaced with a linear fit. The relative movement of head to upper body was used to define maximal ROM. When combining head and eye movement, head rotation relative to space was considered. Gaze was calculated as the sum of the filtered and adjusted head and EOG signals. Repetitions where drift, blinking or artifacts from muscle activity could not be removed successfully from EOG data, were excluded from further analyses (46 of a total of 240 repetitions, asymptomatic group, 10 of 72 repetitions in the symptomatic subjects).

9.5 System precision

The precision of the optical motion capture system in Papers I-IV was estimated by measuring a calibration wand with two markers with a known distance (300 mm). The standard deviation was 0.8 mm in Papers I-II and 1.7 mm in Paper III-IV. In Papers III-IV, the standard deviation was used to simulate Gaussian white noise. Simulated rotations of the head cluster of 1°, 5° and 45 ° with white noise added resulted in calculated helical angles 1.3 ± 0.4°, 5.0 ± 0.4°, and 45.0 ±0.4°, respectively.

The precision of the head motion sensors used in Paper V was high, with high cross-correlations (0.99-0.97) and low average root mean square errors (0.7-2.5°) for simultaneous measurements with a Fastrak system (Jasiewicz et al., 2007).

The horizontal eye movements were measured with EOG. This method has some disadvantages, such as slow DC drift and disturbances from muscle activity. With appropriate filtering and calibration, the accuracy is about 2° (North, 1965).

9.6 Reliability of kinematical calculations

In paper I-II; marker positions were only used for monitoring the rotation of the head. Thus, the exact anatomic position was not so important and was allowed to vary between subjects as long as the rotation was well described by the group of markers. Angle calculations are much more exact when using clusters than when using only single markers, e.g. an error in the calculated angle due to a momentarily hidden marker is reduced. A four-markers-cluster, comparable to the ones used in Papers I-IV, with an error of up to 2 cm in one of the markers position, gives an error in the calculated helical angle that is smaller than 1° (Öhberg, 2008). Position and direction of the axis are more error prone than the angle (Woltring et al., 1985). However, average ICC showed a moderate to high internal reliability in the calculated movement variables. (Paper V). In addition, a pilot test-retest study of six healthy subjects showed a high test-retest reliability of all helical axis variables used in the included studies (θ,$d\theta/dt$, $\mathbf{n}$, $\mathbf{c}$, $\mathbf{CR}$, ω)

with no effects from day of measurement (Grip and Öhberg, 2008, *Submitted*).

Variables describing combined head-eye co-ordination had moderate to high trial-to-trial repeatability (Single ICC>0.4, 31 of 34 variables, Paper V). In general, the average ICC was high (>0.7, 29 of 34 variables). Hence, a mean value of at least three repetitions is recommended to receive reliable output variables. Several repetitions are also recommended since eye blinking and muscle activity artefacts can cause problems when analysing EOG signals (for example in our study 46 of 240 repetitions had to be excluded).

9.7 Statistical methods and pattern classification

The statistical package SPSS for Windows (SPSS, Inc., Il, Chicago, USA, version 10.0 in Papers I-II and version 11.0.1 in Papers III-IV) was used for all statistics. The level of statistical significance was set to $p < 0.05$ in all statistical tests. Partial least squares regression, PLS, was done using SIMCA-P (Umetrics, Inc., version 8.0, Umeå, Sweden), and MATLAB (Mathworks Inc., Natick MA, version 7.1) was used for network classification algorithms.

9.7.1 Group comparisons

Each subject's variable score was calculated as an average of 5 repetitions (Paper I-IV) or 3 repetitions (Paper V). In Paper IV-V, the subject's average was further controlled by regarding single variable scores deviating > 2 SD as outliers and removing them before calculating the subject's average. Right and left side rotations were pooled, and right and left side catching. When calculating **CR**, finite axis from two repetitions were pooled (flexion number 1 with flexion number 2, right side rotation number 1 with left side rotation number 1, etc.). In Paper I, a non-parametric two-sided statistical method (Mann-Whitney U-test) was used for group comparisons. In Paper III-IV, univariate ANOVA was used to test the equality of group means for the three groups (CON, WAD, NP). To ensure that the basic assumptions for ANOVA were fulfilled, Levene's test of equality

of error variances was used. If the test was significant, the variable was transformed using natural logarithm. In addition, Tukey post hoc tests were performed. Correlations between variables and pain intensity were tested using Pearson's correlation coefficient (coefficient given as "R"). In Paper IV, a repeated-measures ANOVA model was used to investigate the migration of $|\mathbf{CR}|$, ω and $|\mathbf{c}|$ over consecutive rotation levels of 15°.

9.7.2 Pattern classification

PLS discriminant analysis was used to evaluate which movement variables that was most important when predicting group membership (Paper I). In addition, a BPNN neural network model was used to classify the movement patterns according to group membership (Paper II). A subject's movement pattern was described by a vector of movement variables. The network structure consisted of one input layer, one hidden layer and one output layer. Two output nodes were used, one represented control subjects and one represented WAD subjects. The node with the highest output signal determined the prediction of the input vector. A leave-one-out method was used in order to keep the training set as large as possible, i.e. the test subject was circulated through the whole data set, and the remaining vectors were divided into a training set (90%) and a validation set (10%). The training set was used for computing the error gradient and updating the network weights and biases with the resilient BP algorithm, and the validation set prevented over-fitting of the BPNN to the training set by using early stopping. A test cycle, i.e., training, validation and testing was done for all 108 subjects. The overall BPNN performance was specified by using the selected BPNN with 100 different initial weights and then calculating the specificity, sensitivity and predictivity.

9.7.3 Internal reliability

Single and average intraclass correlation coefficients, ICC, were used to evaluate internal reliability of the measurements (Study IV-V). ICC>0.4 was regarded as moderate and ICC>0.7 as high correlation (Fleiss, 1986).

10 Results and discussion

10.1 Subjects

In all studies, the neck pain patients scored significantly higher on all questionnaires regarding pain and disability as compared with controls (Table 10.1). In addition, the WAD group clearly suffered from more extensive impairments than the NP group (Papers III-IV): their range of movement was lower (Table 10.2), they scored higher in NPAD, DRI and NDI indices and had a lower self-estimated health status according to EQ-VAS. VAS scores indicated a difference in pain localization between the two groups: shoulder pain intensity was equal, while WAD subjects reported a higher degree of neck pain (Table 10.1). Fear avoidance beliefs were almost equal. All this shows the need to further investigate both neck pain groups.

Table 10.1. Questionnaires reporting pain intensity, fear avoidance and disability in subjects in Papers I-IV. Significant group differences are listed under p-value (* indicates $p<0.05$)

	CON	NP	WAD	p-value	Paper
NPAD	-	-	55 ± 17		I[$]
NPAD	-	36 ± 19	60 ± 17		III-IV
EQ-VAS	88 ± 8	70 ± 18	48 ± 21	* all tests	III-IV
VAS neck	1 ± 2	50 ± 21	66 ± 19	* all tests	III-IV
VAS shoulder	4 ± 8	46 ± 24	54 ± 25	WAD-NP: 0.17 NP-CON* WAD-CON*	III-IV
FABQ Work	-	16 ± 15	23 ± 9	0.06	III-IV
FABQ Phys	-	11 ± 6	13 ± 6	0.54	III-IV

[$]Presented in (Öhberg and Grip, 2003)

10.1.1 External validity

The WAD subjects in Papers I-II consisted of all patients that attended the hospital due to neck trauma during a continuous period of time. Those patients were classified as WAD of different grades by a physician with extensive experience with this patient group. Therefore, this group is considered as a representative sample of WAD patients. In Papers III-IV the neck pain groups consisted of about 20 subjects. Even though the groups were smaller, it is reasonable to believe that they represented selections of the more severe cases with respect to pain intensity and sick leave because they had been referred to rehabilitation clinics and medical centres. In addition, group mean of NPAD was similar in both WAD groups (Table 10.1). In Paper V, six WAD subjects were selected for case studies and hence they were not a representative group. Instead they were carefully chosen based on criteria that would be expected in subgroups of neck pain patients with eye movement abnormalities.

10.2 Head and neck kinematics

A reduced ROM is an inclusion criterion for the neck pain diagnosis. As expected, ROM, but also head velocity were significantly decreased in the neck pain groups as compared with controls in all studies (Table 10.2). In Paper I, it was showed that mean and maximum angular velocity together with decreased ROM and increased reaction times in the different directions explained nearly half of the variance (45%) among the subjects. The velocity variables were the most important to discriminate between individuals with WAD and controls. Therefore, ROM is not the only kinematic variable that should be examined.

10.2.1 Repositioning errors

The repositioning error is probably linked to sensory information from the extensive muscular and articular proprioceptive system in the neck (Heikkilä and Åström, 1996; Kristjansson et al., 2003; Treleaven et al., 2003). Hence, increased repositioning errors were expected in the neck pain groups. However in Paper I, instead the WAD group had significantly smaller repositioning errors for flexion and extension of the neck, while no group

differences were found in axial rotations. The conclusion was that the ability to return to the starting position after each movement depends on velocity, and that slow and controlled movements are required when studying the proprioceptive ability. That was investigated in Paper III during slow movements back to neutral position with eyes closed. No group differences were found (Table 10.2) except for a constant error during flexion, where the WAD group overshot the target as compared with the CON group (-1.8±2.9° vs. 0.1 ±2.4°). In general the repositioning errors were small, comparable in magnitude to observations in other studies (Heikkilä and Åström, 1996; Kristjansson et al., 2003; Treleaven et al., 2003). The repositioning error are larger in neck pain patients that report dizziness (Treleaven et al., 2003), something that was not taken into consideration in the study design. In conclusion, the repositioning error should be studied in combination with other kinematical parameters, and may not be present in all cases of neck pain.

10.2.2 Irregularities in helical axis movement

In addition to the repositioning error, the quality of a performed movement task might be of great clinical importance since the proprioceptive system corrects movements on a moment-to-moment basis (Kristjansson et al., 2003). It was hypothesized that irregularities in the helical axis movement could be such a quality measure. Three such variables were defined: the total trajectory of **c**, the standard variation in ω and the zero-crossing rate of **n** and **c**. A significantly increased irregularity was found during fast head rotations in all movement directions, during head repositioning (side rotation) and during ball catching (Papers III-IV), Table 10.2 and Fig. 10.1. This could imply deficiencies in motor control and proprioceptive function. This is in agreement with studies finding a different activation of the inner musculature of the neck (Falla et al., 2004b), which contains a large number of muscle spindles that mediate proprioception (Boyd-Clark et al., 2002). A higher group SD in zero-crossing rate was observed in the neck pain groups as compared with the healthy controls (Paper IV). Similar results are found in EMG-activity studies, i.e. different chronic pain diagnoses are associated with different changes in EMG activity (Arendt-Nielsen et al., 1996; Fredin et

al., 1997). Moreover there seems to be heterogeneity among subjects with a certain chronic pain diagnosis (Elert et al., 2001). These factors taken together could contribute to the higher SD in the groups with pain in the present study.

10.2.3 Helical axis position, direction and rotation centre

The helical axis was not constant in position and direction, but changed during head movement. It migrated downwards during flexion/extension and axis direction increased towards the end of flexion, extension and side rotation (Paper IV). During slow flexion repositioning (Paper III) the axis was positioned 14.5±2.0 cm above the suprasternal notch in the CON group, and about 2 cm lower in the neck pain groups, Table 10.2. This could relate to limited flexion/extension ability in upper cervical spine. It could also relate to a recruitment of all cervical vertebrae during flexion/extension in the neck pain groups to stabilize the head/neck. Such a strategy may be enhanced when visual information is lacking, since this axis displacement was not observed for the same subject groups during fast head movements with eyes open.

During slow repositioning (Paper III), the anterior component of **n** tended to be larger in the WAD and NP groups. This may indicate a changed curvature of the spine and/or more lateral bending in this group. This can be compared with Lee and co-workers, who found an anterior displacement of the axis of rotation during full flexion/extension in patients with spine instability (Lee et al., 1997).

During fast side rotations, the WAD group showed a superior position of **CR** as compared with the controls (Paper IV), Table 10.2. This could relate to a lower contribution from lower cervical vertebrae, giving a higher **CR** and a lower ROM. In general, **CR** was lower during flexion/extension than during side rotations, which could relate to the fact that flexion/extension is almost equally divided over the cervical vertebrae. During catching, **CR** had its lowest position (Table 10.2). One reason could be that the head had to be stabilized as both upper body and arms were moving, and that the movement in upper cervical spine (C1 and

C2) therefore was restricted. This is in agreement with Moore and co-workers who observed a downward shift of the helical axis during standing (with upper body unsupported) as compared with sitting (Moore et al., 2005).

Higher group SDs was observed in both neck pain groups as compared with the control group in **CR** (Paper IV). This implied individual differences among individuals with neck pain, which can relate to the fact that both non-specific neck pains and whiplash associated pain (WAD) are non-homogenous patient groups, as discussed in 10.2.2.

10.3 Case studies on head-eye co-ordination

In the healthy volunteers, the velocity gain (ratio of eye and head velocity) was close to unity as expected, and the head stability was high during eye-head coordination (group average below 1° head rotation while eyes moved). Range of movement during gaze fixation was about 40° which was lower than ROM without gaze restrictions (Table 10.2). Since the eyes reached on average 90-95% of their maximal range during this task, and since the natural visual range is about 50° (Land, 2006), the visual range probably was the upper limit.

Three of six whiplash subjects lost gaze fixation before the eyes reached 95% of maximal range, even though head rotation was below the subject's ROM without gaze restrictions. This implied a limited eye movement range within which the gaze could be kept fixed, as compared with the asymptomatic group. Three WAD subjects showed difficulties to keep their head still when moving their eyes, as exemplified in Fig. 10.2. No signs of changed velocity gain during gaze fixation or head-eye co-ordination was observed in the six whiplash subjects. Hence, a decreased ROM during gaze fixation, the amount of head movement during head-eye co-ordination, and decreased head velocity when performing the tasks would appear to be of most interest. A more extensive study will be required to determine the repeatability and reliability of the test between days and the

ability of the test to measure changes in response to injury or rehabilitation.

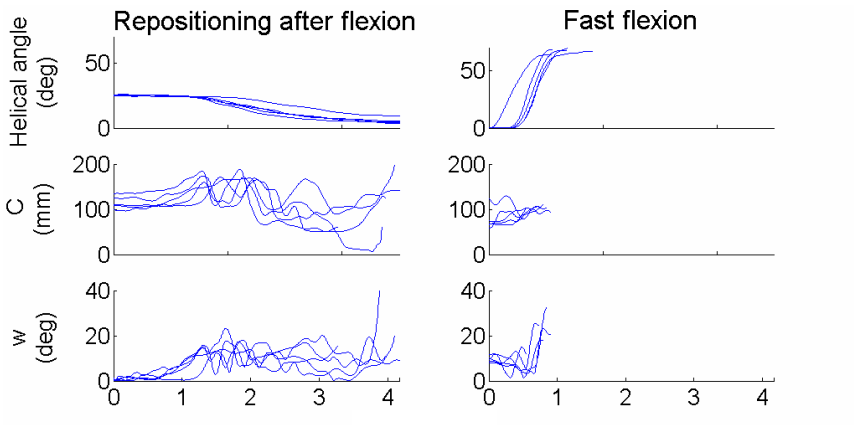

Fig 10.1 Angle of rotation (top), helical axis position (middle) and helical axis direction ω (bottom) during slow repositioning after flexion (A) and fast flexion (B) in a neck pain subject. The horizontal axis represent the time in seconds. Five repetitions are illustrated.

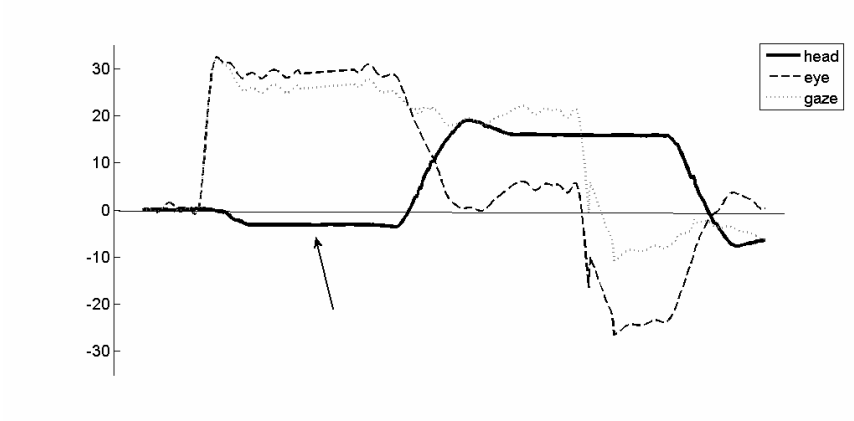

Fig 10.1 Example on head-eye co-ordination in a WAD subject. Three repetitions are illustrated. The arrows mark the shift in head position as the gaze shift from the centre dot to the outer dot on the wall.

Table 10.2 Some results on head and neck kinematics in Papers I-V. Column C indicates condition (F: fast head movement, S: slow head repositioning, B: ball catching, G: gaze fixation, C: Clinical ROM). Column D indicates direction of movement (Si: pooled side rotation, Ri: side rotation to right, Le: Side rotation to left, Fl: flexion, Ex: extension). Significant group differences are listed under p-value (* indicates $p<0.05$). The last column refers to the Paper in which the results are reported.

	C	D	CON	NP	WAD	p-value	In:
ROM (°)	F	Si	72±7		56±15	*	I
		Fl	59±10	_	41±15	all tests	
		E	50±9		31±12		
	C	Si	68±9	55±13	44±13	*	III
		Fl	61±12	52±17	38±18	all tests	
		Ex	59±14	44±18	30±19		
		Ri	62 ±12	_	_		V
		Le	64 ±13				
	G	Ri	41 ± 7	_	_		V
		Le	43 ± 6				
Mean velocity (°/s)	F	Si	135±60		61±35	*	I
		Fl	92±33	_	39±20	all tests	
		Ex	89±38		31±18		
	F	Si	95±30	60±39	43±30	*	IV
		Fl	72±22	45±30	28±23	all dir	
		Ex	59±21	38±24	22±16		
Abs. error (°)	S	Ri	3.1±1.3	2.8±1.2	3.4±1.6	-	III
		Le	3.5±1.3	3.7±1.6	3.7±1.9		
		Fl	2.9±0.9	2.8±1.2	3.4±1.6		
		E	2.7±1.0	2.9±1.3	3.5±1.8		
Cz (cm)	S	Fl	14.5±2.0	12.9±2.1	12.0±1.6	Fl: NP-CON* WAD-CON*	III
		Ex	15.2±2.3	14.5±2.6	14.0±2.8		
c zero crossing (s^{-1})	F	Si	0.8±0.3	1.0±0.3	1.4±0.7	NP-WAD* WAD-CON*	IV
n zero crossing (s^{-1})	F	Si	0.5±0.3	0.6±0.2	0.9±0.6	NP-WAD* WAD-CON*	IV
C traj (cm)	S	L	7.6±5.2	14.0±12.1	15.4±15.9	_	III
		R	6.2±4.2	11.7±18.7	8.3±6.5		
SD ω (°)	S	L	2.3±1.9	4.0±1.7	3.7±2.4	Le: NP-CON* WAD-CON*	III
		R	2.8±1.6	3.2±1.7	3.0±2.0		
CR vertical	F	Si	12.3±4.5	16.1±3.7	15.6±5.8	Side: NP-CON*	IV
		Fl/Ex	11.2±1.4	12.1±2.0	12.6±2.3		
	B	-	8.7±2.0	8.1±2.9	6.8±2.5	_	IV

10.4 Movement analysis as a diagnosis tool

In Papers I-II, it was demonstrated that an objective movement analysis could be used to discriminate between individuals with WAD and controls with high accuracy during rapid head movement in four movement directions. Pattern classification with a BPNN model gave a predictive ability of nearly 90 percent. The tests did not cause any long-term increase of the symptoms in any of the participating subjects (20% recovered within 24 hours and 100% within three days). This is important if the system is going to be used during follow-up and for obvious ethical reasons.

No considerations were made regarding each subject's grade of WAD in Papers I-II. Different clinical methods for grading WAD exist, often with inconsistent results. From the healthcare provider's point of view, it is desirable to grade WAD into sub classes, related to different pathogenesis, pain mechanisms and long-term outcome (e.g., ability to work) in a more distinct manner than the grading of WAD proposed by the Quebec Task Force. A reasonable next step would be to identify subclasses of WAD patients. This could enhance the development of more precise diagnostic procedures for WAD patients. Hence, to get more detailed information about head motility (such as head-eye co-ordination, quality of the performed movement, position of the axis of motion during different movement conditions), other variables must be recorded in addition to head ROM.

Papers I-IV showed group differences in other kinematic variables than ROM (Table 10.2) but also individual differences within the group of neck pain patients. Repositioning errors were small and should be viewed in combination with other variables. Case studies of WAD patients with visual problems indicated that the head-eye co-ordination tests may used to investigate deficits in gaze fixation and head-eye co-ordination in sub groups of neck pain patients.

To conclude, kinematic analysis of several variables on head and neck movement, possibly in combination with eye and upper body movement, could give detailed information that could be useful during diagnosing and follow-up of neck pain patients.

Pattern classification can be used to discriminate between individuals. However, knowledge about what variables to look at, and interpretation of each variable is required in addition. For clinical settings, a simple and preferably portable motion capture system is needed, even though an optical motion capture system is very accurate and thus suitable for research and laboratory settings.

10.5 Implications for further research

Further research should be done on portable motion systems such as wireless motion sensors since they could be incorporated as a portable system with possible clinical applications. The reliability of calculated helical axis variables derived from data registered with such motion systems should be investigated. Probably an instantaneous approach would be more appropriate than a finite approach if the registered data are in the form of angular velocity and linear acceleration (as when using motion sensors) rather than marker positions (as when using optical motion capture systems).

Case studies on patients with known localisation of spinal injuries (for example, if such are found with X-ray or MR) should be examined to investigate relations between those injuries and helical axis characteristics. Axis orientation of individual vertebrae might be localized, and could be used to study if single vertebral defects have an effect on the global helical axis location. That could give implications on underlying mechanisms behind abnormalities in the global helical axis.

Combined analysis of several movement variables should be further investigated. Since eye movement disturbances are expected in specific subgroups of neck pain patients, combined head and eye movement should be investigated further on both healthy controls and subjects with neck pain. If the method is effective, a portable system might include EOG measurements. In addition, parameters describing muscle activity might give additional information. For example, other studies implies a change in co-ordination between deep and superficial neck musculature and changes in muscle activity pattern (Falla et al.,

2004; Falla et al., 2004b; Fredin et al., 1997; Treleaven et al., 2003).

Finally, the methods used in this dissertation have a large potential for generalisation to other areas than head kinematics such as hip, knee and shoulder movements.

11 Conclusions

1) Biomechanical methods and models were further developed in order to analyse head and neck movement. Specifically:
   - The methods and models used in this thesis gave accurate measurements of head and neck movement, e.g. of movement range, velocity, reaction time and movement symmetry parameters.
   - A modified finite helical axis method with a variable time window ($\Delta\theta$=4°), gave valuable information about the cervical helical axis. Increased irregularity in the helical axis movement, a displaced position of the axis and its centre of rotation implies that this method is sensitive enough to describe disturbed neck movement patterns in neck pain patients.
   - Simultaneous measurements of head and eye movement may give information about disturbed head-eye co-ordination, but needs further investigation.

2) Even though severe cases existed in both neck pain groups, individuals with whiplash seemed to have more severe disturbances than individuals with non-specific neck pain (NP). Specifically:

- The WAD group generally scored higher in pain and disability indices then the NP group, but not in indices describing fear avoidance.
- In addition they had a smaller movement range and slower mean velocities during head movement, probably as a consequence from pain and disability.
- They had a larger amount of irregularities in helical axis position and direction and signs on larger repositioning errors, which could relate to more a more disturbed sensorimotor control system, e.g. from a reduced proprioceptive ability.

3) Kinematical analyses of head and neck movement have a potential to be used as a decision support for physicians and physiotherapists during diagnosis and follow-up of neck pain patients. Specifically:

- Objective movement analysis gives valuable, objective information about head movement patterns that are difficult to find by visual inspection.
- Some variables are not sufficient as single indicators, such as the repositioning error. In addition, several different subgroups probably exist within the heterogeneous group of neck pain patients. Therefore, several different aspects of head kinematics should be studied. Multivariate pattern classification models emphasized that a combined analysis of several kinematical variables would most accurately discriminate between individuals with and without neck pain.
- An optical motion capture system gives accurate and reliable measurements in a laboratory environment, but a flexible and user friendly motion capture system is needed to perform measurements at a clinic or in a home environment. The motion sensors used in Study V have that potential.

Acknowledgements

There are many people among my colleages, friends and relatives that I would like to express my gratitude for. A complete list would be impossible, but I want to mention some of you who have been especially important for me during this time:

Stefan Karlsson, my head supervisor, who introduced me into the field of biomedical research with lots of enthusiasm and knowledge. You have an amazing ablity to see things in a larger perspective and you have always been encouraging and helpful. I have appreciated your support and our discussions about present and future research a lot.

Gunnevi Sundelin and Björn Gerdle, my co-supervisors. You have given me invaluable help during the last years, and I have learned a lot from your extensive experience within the field of research and medicine.

Fredrik Öhberg, co-author, for good teamwork, insightful comments on my papers and discussions about this research in general.

All my co-workers at the R&D unit at the Department of Biomedical Engineering. The friendly and creative atmosphere makes it easy to come to work. I especially want to thank Nina, Marcus, Markus, and Tomas - Tomas and Markus for skilled help and guidance in the construction of some of the electronic equipment, Marcus for many hours at cimbing walls, and all of you for friendship, for all kinds of enjoyable tours and events, and for discussions about all and nothing.

Monica Edström – I appreciated your assistance and enjoyed all the small talking during hours of data collection. And all my other

colleagues at the Department of Community Medicine and Rehabilitation for inspiring collaboration.

Leif and Lennart Nilsson at the Department of Mathematics and Mathematical Statistics, for advices about statistical analysis.

Gwendolen Jull and Julia Treleaven, for welcoming me to the whiplash clinic at the University of Queensland. You were friendly and helpful during my three months intensive stay in Brisbane, and I am grateful that you took the time to share your knowledge about whiplash. It was invaluable.

Everyone who participated in my studies - of course I could not have done this without your participation.

Ania with Chorall, for pleasant and important breaks with music and singing.

My friends and my family for support and inspiration – and for putting up with me the last months, even though I have been even more unorganized then usual (yes, it was possible!). Especially Karolina, Taina and Birgitta for being such close and dear friends - thanks for lots of laughter and crazy adventures and your ability to appreciate the good things in life. Tove, Bambi, Jenny, Maria, Ewa, Håkan and all the rest of you.... I hope you know that you are important to me!

Finally, of course, Thomas, for your love, kindness, patience and support at all times.

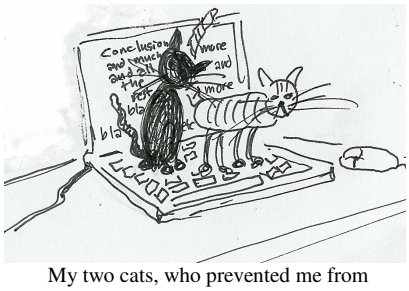

My two cats, who prevented me from working too much by sitting on my laptop.

References

Alanko HI. 1984. Clinical electro-oculography. Acta Ophthalmol Suppl 161:139-148.

Amevo B, Aprill C, Bogduk N. 1992. Abnormal instantaneous axes of rotation in patients with neck pain. Spine 17:748-756.

Amevo B, Worth D., N. B. 1991. Instantaneous axes of rotation of the typical cervical motion segments: a study in normal volunteers. Spine 6:111-117.

Antonaci F, Ghirmai S, Bono G, Nappi G. 2000. Current methods for cervical spine movement evaluation: a review. Clin Exp Rheumatol 18:S45-52.

Arendt-Nielsen L, Graven-Nielsen T, Svarrer H, Svensson P. 1996. The influence of low back pain on muscle activity and coordination during gait: a clinical and experimental study. Pain 64:231-240.

Ariens GA, van Mechelen W, Bongers PM, Bouter LM, van der Wal G. 2001. Psychosocial risk factors for neck pain: a systematic review. Am J Ind Med 39:180-193.

Barnsley L, Lord SM, Wallis BJ, Bogduk N. 1995. The prevalence of chronic cervical zygapophysial joint pain after whiplash. Spine 20:20-25; discussion 26.

Bernard BE. 1997. Musculosceletal disorders and workplace factors. In: National Institute for Occupational Safety and Health. p 2:1-22.

Bogduk N. 1984. Neck pain. Aust Fam Physician 13:26-30.

Bogduk N. 1988. Neck pain: an update. Aust Fam Physician 17:75-80.

Bogduk N, Marsland A. 1988. The cervical zygapophysial joints as a source of neck pain. Spine 13:610-617.

Bonuccelli U, Pavese N, Lucetti C, Renna MR, Gambaccini G, Bernardini S, Canapicchi R, Carrozzi L, Murri L. 1999. Late whiplash syndrome: a clinical and magnetic resonance imaging study. Funct Neurol 14:219-225.

Borghouts JA, Koes BW, Bouter LM. 1998. The clinical course and prognostic factors of non-specific neck pain: a systematic review. Pain 77:1-13.

Boyd-Clark LC, Briggs CA, M.P. G. 2002. Muscle spindle distribution, morphology,and density in the longis colli and multifidus muscles of the cervical spine. Spine 27:694-701.

Brown M, Marmor M, Vaegan, Zrenner E, Brigell M, Bach M. 2006. ISCEV Standard for Clinical Electro-oculography (EOG) 2006. Doc Ophthalmol 113:205-212.

Carlsson A-M. 1983. Assessment of chronic pain. I. Aspects of the reliability and validity of the visual analogue scale. Pain 16:87-101.

Carlsson I, Hedin M, Brorsson J, Gårdestig S, Lundgren M, Rehnqvist N, Danielsson H, Lundius A. 2005. The Whiplash Commission Final Report. In. Sandviken, Sweden.

Coley B, Najafi B, Paraschiv-Ionescu A, Aminian K. 2005. Stair climbing detection during daily physical activity using a miniature gyroscope. Gait Posture 22:287-294.
Corneil BD, Olivier E, Munoz DP. 2002. Neck muscle responses to stimulation of monkey superior colliculus. I. Topography and manipulation of stimulation parameters. J Neurophysiol 88:1980-1999.
Crowe. 1928. Injuries to the cervical spine.
Daffner RH. 2001. Identifying patients at low risk for cervical spine injury: the Canadian C-spine rule for radiography. Jama 286:1893-1894.
Duda R, Hart PE, Stork DG. 2001. Unsupervised learning and clustering. In: Pattern Classification. Danvers, MA: John Wiley&Sons,Inc.
Elert J, Kendall SA, Larsson B, Mansson B, Gerdle B. 2001. Chronic pain and difficulty in relaxing postural muscles in patients with fibromyalgia and chronic whiplash associated disorders. J Rheumatol 28:1361-1368.
Eren H. 1999. Acceleration, vibration and shock measurement, Chapter 17. In: Webster JG, editor. Measurement, Instrumentation and sensors. Danvers MA USA: CRC Press LLC.
Eriksson L. 1999. Introduction to Multivariate and Megavariate Data ANalysis using Projection Methods (PCA and PLS). Umeå, Sweden: Umetrics AB.
Falla D, Bilenkij G, Jull G. 2004. Patients with chronic neck pain demonstrate altered patterns of muscle activation during performance of a functional upper limb task. Spine 29:1436-1440.
Falla D, Jull G, Hodges P. 2004b. Patients with neck pain demonstrate reduced electromyographic activity of the deep cervical flexor muscles during performance of the craniocervical flexion test. Spine 29:2108-2114.
Falla D, Jull G, Rainoldi A, Merletti R. 2004. Neck flexor muscle fatigue is side specific in patients with unilateral neck pain. Eur J Pain 8:71-77.
Favre J, Jolles BM, Aissaoui R, Aminian K. 2008. Ambulatory measurement of 3D knee joint angle. J Biomech.
Feipel V, Rondelet B, Le Pallec J, Rooze M. 1999. Normal global motion of the cervical spine: an electrogoniometric study. Clin Biomech (Bristol, Avon) 14:462-470.
Fjellman-Wiklund A, Sundelin G. 1998. Musculoskeletal discomfort of music teachers: an eight-year perspective and psychosocial work factors. Int J Occup Environ Health 4:89-98.
Fleiss JL. 1986. The design and analysis of clinical experiments. New York: Wiley.
Fredin Y, Elert J, Britschigi N, Vaher A, Gerdle B. 1997. A decreased ability to relax between repetitive muscle contractions in patients with chronic symptoms after whiplash trauma of the neck. J Musculoskel Pain 5:55-70.
Gerdle B, Lemming D, Kristiansen J, Larsson B, Peolsson M, Rosendal L. 2008. Biochemical alterations in the trapezius muscle of patients with

chronic whiplash associated disorders (WAD) - A microdialysis study. Eur J Pain 12:82-93.
Giansanti D, Macellari V, Maccioni G, Cappozzo A. 2003. Is it feasible to reconstruct body segment 3-D position and orientation using accelerometric data? IEEE Trans Biomed Eng 50:476-483.
Gimse R, Tjell C, Bjorgen IA, Saunte C. 1996. Disturbed eye movements after whiplash due to injuries to the posture control system. J Clin Exp Neuropsychol 18:178-186.
Golub GH, van Loan CF. 1983. The QR Factorization. In: Matrix Computations. Baltimore, Maryland: The John Hopkins University Press. p 211-221.
Golub GH, van Loan CF. 1983. The symmetric Eigenvalue problem. In: Matrix Computations. Baltimore, Maryland: The John Hopkins University Press.
Gray H. 1918. Anatomy of the Human Body. Philadelphia: Lea & Febiger.
Grip H, Ohberg F, Wiklund U, Sterner Y, Karlsson JS, Gerdle B. 2003. Classification of neck movement patterns related to whiplash-associated disorders using neural networks. IEEE Trans Inf Technol Biomed 7:412-418.
Grip H, Sundelin G, Gerdle B, Karlsson JS. 2007. Variations in the axis of motion during head repositioning--a comparison of subjects with whiplash-associated disorders or non-specific neck pain and healthy controls. Clin Biomech (Bristol, Avon) 22:865-873.
Grip H, Sundelin G, Gerdle B, Karlsson JS. 2008a, *Submitted*. Cervical helical axis characteristics and its center of rotation during active head movements - comparisons of whiplash-associated disorders, non-specific neck pain and asymptomatic individuals.
Grip H, Treleaven J, Jull G. 2008b, *Submitted*. Head eye co-ordination and gaze stability using simultaneous measurement of eye in head and head in space movements - potential for use in subjects with a whiplash injury.
Grip H, Öhberg F. 2008, *Submitted*. Test-retest reliability of variables describing head movement characteristics - A 3D movement analysis using the Helical Axis Method, In: International Society of Biomechanics Conference, Ann Arbor, Michigan, USA
Heikkilä H, Åström PG. 1996. Cervicocephalic kinesthetic sensibility in patients with whiplash injury. Scand J Rehabil Med 28:133-138.
Heikkilä HV, Wenngren BI. 1998. Cervicocephalic kinesthetic sensibility, active range of cervical motion, and oculomotor function in patients with whiplash injury. Arch Phys Med Rehabil 79:1089-1094.
Heller CA, Stanley P, Lewis-Jones B, Heller RF. 1983. Value of x ray examinations of the cervical spine. Br Med J (Clin Res Ed) 287:1276-1278.
Hinderaker J, Lord SM, Barnsley L, Bogduk N. 1995. Diagnostic value of C2-3 instantaneous axes of rotation in patients with headache of cervical origin. Cephalalgia 15:391-395.

Hopfield JJ. 1982. Neural networks and physical systems with emergent collective computational abilities. Proc Natl Acad Sci U S A 79:2554-2558.

Ingster-Moati I, Bui Quoc E, Pless M, Djomby R, Orssaud C, Guichard JP, Woimant F. 2007. Ocular motility and Wilson's disease: a study on 34 patients. J Neurol Neurosurg Psychiatry 78:1199-1201.

Ishii T, Mukai Y, Hosono N, Sakaura H, Nakajima Y, Sato Y, Sugamoto K, Yoshikawa H. 2004. Kinematics of the upper cervical spine in rotation: in vivo three-dimensional analysis. Spine 29:E139-144.

Jasiewicz JM, Treleaven J, Condie P, Jull G. 2007. Wireless orientation sensors: their suitability to measure head movement for neck pain assessment. Man Ther 12:380-385.

Jull G, Kristjansson E, Dall'Alba P. 2004. Impairment in the cervical flexors: a comparison of whiplash and insidious onset neck pain patients. Man Ther 9:89-94.

Kamibayashi LK, Richmond FJ. 1998. Morphometry of human neck muscles. Spine 23:1314-1323.

Kerr D, Bradshaw L, Kelly AM. 2005. Implementation of the Canadian C-spine rule reduces cervical spine x-ray rate for alert patients with potential neck injury. J Emerg Med 28:127-131.

Khoshnoodi MA, Motiei-Langroudi R, Omrani M, Ghaderi-Pakdell F, Abbassian AH. 2006. Kinesthetic memory in distance reproduction task: importance of initial hand position information. Exp Brain Res 170:312-319.

Kogler A, Lindfors J, Odkvist LM, Ledin T. 2000. Postural stability using different neck positions in normal subjects and patients with neck trauma. Acta Otolaryngol 120:151-155.

Kristjansson E, Dall'Alba P, Jull G. 2003. A study of five cervicocephalic relocation tests in three different subject groups. Clin Rehabil 17:768-774.

Kulkarni V, Chandy M, Babu K. 2001. Quantitative study of muscle spindles in suboccipital muscles of human foetuses. Neurology India 49:355 - 359.

Land MF. 2006. Eye movements and the control of actions in everyday life. Prog Retin Eye Res 25:296-324.

Lee SW, Draper ER, Hughes SP. 1997. Instantaneous center of rotation and instability of the cervical spine. A clinical study. Spine 22:641-647; discussion 647-648.

Malmstrom EM, Karlberg M, Melander A, Magnusson M. 2003. Zebris versus Myrin: a comparative study between a three-dimensional ultrasound movement analysis and an inclinometer/compass method: intradevice reliability, concurrent validity, intertester comparison, intratester reliability, and intraindividual variability. Spine 28:E433-440.

Mayagoitia RE, Nene AV, Veltink PH. 2002. Accelerometer and rate gyroscope measurement of kinematics: an inexpensive alternative to optical motion analysis systems. J Biomech 35:537-542.

McColough WS, Pitts WH. 1943. A logical calculus of the ideas immanent in nervous activity. Bulletin of Mathematical Biophysics 5:115-133.
Mellin G. 1986. Measurement of thoracolumbar posture and mobility with a Myrin inclinometer. Spine 11:759-762.
Mergner T, Schweigart G, Botti F, Lehmann A. 1998. Eye movements evoked by proprioceptive stimulation along the body axis in humans. Exp Brain Res 120:450-460.
Michaelson P, Michaelson M, Jaric S.L. LM, P. S, Djupsjöbacka M. 2003. Vertical posture and head stability in patients with chronic neck pain. Journal of Rehabilitation Medicine 35:229-235.
Miettinen T, Leino E, Airaksinen O, Lindgren KA. 2004. Whiplash injuries in Finland: the situation 3 years later. Eur Spine J 13:415-418.
Milne N. 1993. Composite motion in cervical disc segments. Clin Biomech (Bristol, Avon) 8:193-202.
Moffett J, McLean S. 2006. The role of physiotherapy in the management of non-specific back pain and neck pain. Rheumatology (Oxford) 45:371-378.
Moore ST, Hirasaki E, Raphan T, Cohen B. 2005. Instantaneous rotation axes during active head movements. J Vestib Res 15:73-80.
Nidecker A, Pernus B, Hayek J, Ettlin T. 1997. ["Whiplash" injury of the cervical spine: value of modern diagnostic imaging]. Schweiz Med Wochenschr 127:1643-1651.
Nigg BM, Cole GK, Wrigth IC. 2003. Optical Methods. In: Nigg BM, Herzog.W., editors. Biomechanics of the Musculo-skeletal System, 2nd ed. Chichester: John Wiley & Sons Ltd.
North AW. 1965. Accuracy and precision of Electro-oculographic recording. Invest Ophthalmol 4:343-348.
Panjabi MM, Pearson AM, Ito S, Ivancic PC, Wang JL. 2004. Cervical spine curvature during simulated whiplash. Clin Biomech (Bristol, Avon) 19:1-9.
Penning L. 1978. Normal movements of the cervical spine. AJR Am J Roentgenol 130:317-326.
Penning L, Wilmink JT. 1987. Rotation of the cervical spine. A CT study in normal subjects. Spine 12:732-738.
Pinney CP, Baker WE. 1999. Velocity measurement -Chapter 16. In: Webster JG, editor. Measurement, Instrumentation and sensors. Danvers MA USA: CRC Press LLC.
Putz R, Pabst R. 1994a. Atlas of Human anatomy, Volume 1 - Head, Neck and Upper Limb, 12th english ed. Munich: Urban & Schwarzenberg.
Putz R, Pabst R. 1994b. Atlas of Human anatomy, Volume 2 - Thorax, Abdomen, Pelvis, Lower Limb, 12th english ed. Munich: Urban & Schwarzenberg.
Qiu TX, Teo EC, Lee KK, Ng HW, Yang K. 2004. Kinematics of the thoracic T10-T11 motion segment: locus of instantaneous axes of rotation in flexion and extension. J Spinal Disord Tech 17:140-146.

Rabin R, de Charro F. 2001. EQ-5D: a measure of health status from the EuroQol Group. Ann Med 33:337-343.
Rosenblatt F. 1958. The Perceptron: A Probabilistic Model for Information Storage and Organization in the Brain. Psychological Review 65:386-408.
Rosendal L, Kristiansen J, Gerdle B, Sogaard K, Peolsson M, Kjaer M, Sorensen J, Larsson B. 2005. Increased levels of interstitial potassium but normal levels of muscle IL-6 and LDH in patients with trapezius myalgia. Pain 119:201-209.
Rumelhart DE, Hinton GE, Williams RJ. 1986. Learning representations by back-propagating errors. Nature 323:533 - 536.
Salen BA, Spangfort EV, Nygren ÅL, Nordemar R. 1994. The disability rating index: An instrument for the assessment of disability in clinical settings. Journal of Clinical Epidemiology 47:1423-1435.
Schlag J, Merker B, Schlag-Rey M. 1983. Comparison of EOG and search coil techniques in long-term measurements of eye position in alert monkey and cat. Vision Res 23:1025-1030.
Scholten-Peeters GG, Verhagen AP, Bekkering GE, van der Windt DA, Barnsley L, Oostendorp RA, Hendriks EJ. 2003. Prognostic factors of whiplash-associated disorders: a systematic review of prospective cohort studies. Pain 104:303-322.
Scott D, Jull G, Sterling M. 2005. Widespread sensory hypersensitivity is a feature of chronic whiplash-associated disorder but not chronic idiopathic neck pain. Clin J Pain 21:175-181.
Senouci M, FitzPatrick D, Quinlan JF, Mullett H, Coffey L, McCormack D. 2007. Quantification of the coupled motion that occurs with axial rotation and lateral bending of the head-neck complex: an experimental examination. Proc Inst Mech Eng [H] 221:913-919.
Spitzer WO, Skovron ML, Salmi LR, Cassidy JD, Duranceau J, Suissa S, Zeiss E. 1995. Scientific monograph of the Quebec Task Force on Whiplash-Associated Disorders: redefining "whiplash" and its management. Spine 20:1S-73S.
Spoor CW, Veldpaus FE. 1980. Rigid body motion calculated from spatial co-ordinates of markers. J Biomech 13:391-393.
Sterner Y, Gerdle B. 2004. Acute and chronic whiplash disorders--a review. J Rehabil Med 36:193-209.
Stiell IG, Wells GA, Vandemheen KL, Clement CM, Lesiuk H, De Maio VJ, Laupacis A, Schull M, McKnight RD, Verbeek R, Brison R, Cass D, Dreyer J, Eisenhauer MA, Greenberg GH, MacPhail I, Morrison L, Reardon M, Worthington J. 2001. The Canadian C-spine rule for radiography in alert and stable trauma patients. Jama 286:1841-1848.
Sundelin G, Hagberg M. 1992. Electromyographic signs of shoulder muscle fatigue in repetitive arm work paced by the Methods-Time Measurement system. Scand J Work Environ Health 18:262-268.
Sundström T, Guez M, Hildingsson C, Toolanen G, Nyberg L, Riklund K. 2006. Altered cerebral blood flow in chronic neck pain patients but

not in whiplash patients: a 99mTc-HMPAO rCBF study. Eur Spine J 15:1189-1195.
Sweetman BJ. 2006. Physiotherapy management of non-specific back and neck pain. Rheumatol (Oxford) 45:1451-1452.
Söderkvist I. 1990. Computation of the screw axis characteristics corresponding to a known movement in R3. In. Umeå: Institute of Information Processing. p 1-14.
Söderkvist I, Wedin PA. 1993. Determining the movements of the skeleton using well-configured markers. J Biomech 26:1473-1477.
Taylor J, Taylor M. 1996. Cervical spinal injuries: an autopsy study of 109 blunt injuries. J Musculoskeletal Pain 4:61-79.
Tian JR, Crane BT, Ishiyama A, Demer JL. 2007. Three dimensional kinematics of rapid compensatory eye movements in humans with unilateral vestibular deafferentation. Exp Brain Res 182:143-155.
Tortora G, Grabowski S. 2000. Principles of anatomy and physiology, 9 ed. New York: John Wiley & sons, Inc.
Treleaven J, Jull G, Sterling M. 2003. Dizziness and unsteadiness following whiplash injury: characteristic features and relationship with cervical joint position error. J Rehabil Med 35:36-43.
Tweed D, Vilis T. 1990. Geometric relations of eye position and velocity vectors during saccades. Vision Res 30:111-127.
Waddell G, Newtona M, Hendersona I, Somervillea D, Mainb CJ. 1992. A Fear-Avoidance Beliefs Questionnaire (FABQ) and the role of fear-avoidance beliefs in chronic low back pain and disability. Pain 52:157-168.
Werner J. 1980. Neuroscience- A clinical perspective, In: Canada
Vernon H, Mior S. 1991. The Neck Disability Index: a study of reliability and validity. J Manipulative Physiol Ther 14:409-415.
Wheeler AH, Goolkasian P, Baird AC, Darden BV. 1999. Development of the Neck Pain and Disability Scale: Item Analysis, Face, and Criterion-Related Validity. Spine 24:1290-1294.
White AA, 3rd, Panjabi MM. 1978. The basic kinematics of the human spine. A review of past and current knowledge. Spine 3:12-20.
Winters JM, Peles JD, Osterbauer PJ, Derickson K, Deboer KF, Fuhr AW. 1993. Three-dimensional head axis of rotation during tracking movements. A tool for assessing neck neuromechanical function. Spine 18:1178-1185.
Woltring HJ, Huiskes R, de-Lange A, Veldpaus FE. 1985. Finite centroid and helical axis estimation from noisy landmark measurements in the study of human joint kinematics. J Biomech 18:379-389.
Woltring HJ, Long K, Osterbauer PJ, Fuhr AW. 1994. Instantaneous helical axis estimation from 3-D video data in neck kinematics for whiplash diagnostics. J Biomech 27:1415-1432.
Wong WY, Wong MS, Lo KH. 2007. Clinical applications of sensors for human posture and movement analysis: a review. Prosthet Orthot Int 31:62-75.

Zatsiorsky VM. 1998. Kinematics of Human Motion. Pennsylvania: Human Kinetics Pub.
Zhou H, Stone T, Hu H, Harris N. 2008. Use of multiple wearable inertial sensors in upper limb motion tracking. Med Eng Phys 30:123-133.
Öhberg F. 2008. The effect of anisotropic systematic errors in estimating helical angles. Comput Methods Biomech Biomed Engin 11:205-213.
Öhberg F, Grip H. 2003. Chronic whiplash associated disorders - Prediction of pain and disability scale using artificial neural networks, In: World Congress on Medical Physics and Biomedical Engineering (WC2003), Sydney, Australia, August 24-29
Öhberg F, Grip H, Wiklund U, Sterner Y, Karlsson JS, Gerdle B. 2003. Chronic whiplash associated disorders and neck movement measurements: an instantaneous helical axis approach. IEEE Trans Inf Technol Biomed 7:274-282.

Appendix

Appendix 1 Singular Value Decomposition

If **R** is a m×n matrix (m≥n), then there exis an orthogonal m×m matrix **U,** an orthogonal n×n matrix **V,** and a diagonal matrix **D** such that

$$\mathbf{U}^T\mathbf{R}\mathbf{V}=\mathbf{D}_A=\text{diag}(\lambda_1, \lambda_2,\ldots \lambda_n)$$

where λ_i is the eigenvalues of **R.** (Golub and van Loan, 1983)

The eigenvalues fulfill $\mathbf{R}\mathbf{e}_i=\lambda_i\mathbf{e}_i$, where $\mathbf{e}_i$ is an eigenvector of **R**, i.e. under muliplication by **R**, an eigenvector is changed only in magnitude, not in direction.

Appendix 2 Principal component analysis

Compute the d-dimensional mean vector $\boldsymbol{\mu}$ and the d×d covariance matrix $\boldsymbol{\Sigma}$ of a n×d dataset (n observations, d dimensions). Compute eigenvalues and eigenvectors (for example by using Singular Value Decomposition), and sort according to decreasing eigenvalue. Choose the *k* eigenvectors that have the largest eigenvalues (often there will be just a few vectors with large eigenvalues). Form a d×k matrix **A** whose columns consists of the *k* eigenvectors. By projecting the data onto the k-dimensional subspace, a principal component presentation of the data: $\mathbf{x'} = \mathbf{A}^T(\mathbf{x}-\boldsymbol{\mu})$ is produced. (Duda et al., 2001)